Contents lists available at ScienceDirect

Biosensors and Bioelectronics

journal homepage: www.elsevier.com/locate/bios

Multiplexed immunosensors for point-of-care diagnostic applications

Bruno Gil Rosa [a], Oluwatomi E. Akingbade [b,c], Xiaotong Guo [d], Laura Gonzalez-Macia [e], Michael A. Crone [c,f], Loren P. Cameron [c,f], Paul Freemont [c,f], Kwang-Leong Choy [g], Firat Güder [e], Eric Yeatman [d], David J. Sharp [b,c], Bing Li [b,c,g,*]

[a] Hamlyn Centre, Imperial College London, London, SW7 2AZ, UK
[b] Department of Brain Science, Imperial College London, London, W12 0BZ, UK
[c] Care Research & Technology Centre, UK Dementia Research Institute, London, W12 0BZ, UK
[d] Department of Electrical and Electronic Engineering, Imperial College London, London, SW7 2AZ, UK
[e] Department of Bioengineering, Imperial College London, London, SW7 2AZ, UK
[f] Section of Structural and Synthetic Biology, Department of Infectious Disease, Imperial College London, London, SW7 2AZ, UK
[g] Institute for Materials Discovery, University College London, Roberts Building, London, WC1E 7JE, UK

ARTICLE INFO

ABSTRACT

Accurate, reliable, and cost-effective immunosensors are clinically important for the early diagnosis and monitoring of progressive diseases, and multiplexed sensing is a promising strategy for the next generation of diagnostics. This strategy allows for the simultaneous detection and quantification of multiple biomarkers with significantly enhanced reproducibility and reliability, whilst requiring smaller sample volumes, fewer materials, and shorter average analysis time for individual biomarkers than individual tests. In this opinionated review, we compare different techniques for the development of multiplexed immunosensors. We review the state-of-the-art approaches in the field of multiplexed immunosensors using electrical, electrochemical, and optical methods. The barriers that prevent translating this sensing strategy into clinics are outlined together with the potential solutions. We also share our vision on how multiplexed immunosensors will continue their evolution in the coming years.

1. Introduction

Immunosensors use antibodies as the biological recognition element to convert an antibody–antigen binding event into a measurable physical signal, which has been a well-established clinical tool for the detection of analytes at low concentrations. This technology benefits from highly specific antibody-antigen binding, which provides sensitive ways to detect a range of biomolecules, such as bacteria, viruses, protein biomarkers, nucleic acids, and other small molecules. To date, many immunosensing systems have been developed to meet the urgent needs of different clinical settings. Enzyme-linked immunosorbent assay (ELISA), the most commonly used method developed in the 1970s (Bange et al., 2005; Kadimisetty et al., 2015), offers sensitivity at picograms per millilitre for the detection of protein biomarkers, but long analysis times, the ability to detect only single analytes, and low sensitivity for many newly discovered biomarkers (Li et al., 2020) are some of the major limitations of ELISA. From the 1980s, lateral flow

immunosensors emerged for the detection of biomarkers at the point-of-care (POC) (Wang et al., 2020). Lateral flow immunosensors offer rapid, semi-quantitative detection of individual biomarkers with a lower sensitivity of sub-nanograms per millilitre and have become one of the most promising methods in primary clinical frontline screening. But they are less sensitive than laboratory ELISAs and incapable of providing accurate quantitative diagnostic information, such as the concentration of biomarkers (Koczula and Gallotta, 2016). Due to this, many other commercial immunosensing systems have been developed with an aim to achieve fast, cost-effective, reliable, and highly sensitive immunosensing, such as Luminex (Wang et al., 2005) and Quansys multiplexed ELISA (Rosser et al., 2014). In the 2010s, a single molecule assay (Simoa) was reported and became the state-of-the-art technology in simultaneously quantifying multiple biomarkers at extremely low concentrations, from sub-picograms to femtograms per millilitre (Rissin et al., 2010). Meanwhile in laboratory environments, proof-of-concept of improved immunosensing systems employing different readout

mechanisms have been increasingly reported. They mainly include optical (e.g., surface plasmon resonance (SPR) (Petrova et al., 2019), surface-enhanced Raman scattering (SERS) (Liu et al., 2018a), fluorescence microscopy (Lee et al., 2019), luminescence detection (Kadimisetty et al., 2018), optical absorbance and colorimetry (Phillips et al., 2018)), magnetic and electrical (e.g., giant magnetoresistance (Gao et al., 2019), field effect transistor (Kim et al., 2020)), and electrochemical sensors (Jirakova et al., 2019; Wan et al., 2013). From these milestone achievements, a multiplexed biosensing strategy has become a focal point for the development of next generation immunosensors. Fig. 1 shows the molecular structure of an antibody (the recognition receptor in immunosensors), different types of analytes that can be detected, and the main measurement methods employed in immunosensing systems.

Biomarkers and their concentrations reflect the biological processes and indicate the presence or severity of the corresponding diseases. However, due to the heterogeneous nature of most diseases, the types and concentrations of most discriminative biomarkers vary at different stages across individuals. This phenomenon is particularly evident in patients with progressive diseases (Dubois et al., 2014), including neurodegenerative diseases (Li et al., 2020), cancer (Chikkaveeraiah et al., 2012), cardiac diseases (Mohammed and Desmulliez, 2011), infectious diseases (Xu et al., 2020) and many other health conditions (Li et al., 2017). Therefore, the detection of one single biomarker alone is usually insufficient to provide enough information for clinical diagnosis or to track the progression of diseases. Multiplexed immunosensors enable the simultaneous detection of a panel of discriminative biomarkers, which can statistically improve the accuracy of detection. In addition, compared with detecting different biomarkers separately, multiplexed immunosensors offer higher throughput, consume less sample and reagents, require less analysis time, and generate highly reproducible sensing signals, as shown in Fig. 2. Although they require complex mathematical algorithms for the simultaneous analysis of multiple biomarkers and the evaluation of signal interferences, the development of multiplexed immunosensors is still an attractive approach for the diagnosis and monitoring of progressive diseases, especially in sample volumes or resource-limited clinical settings. They will also facilitate the development of disease modifying treatments,

preventive strategies, and effective drug discovery.

To date, thousands of "multiplexed immunosensing"-related articles have been published, but the development of clinically useful multiplexed immunosensors is still in its infant stage. There is an urgent need to further develop multiplexed immunosensors for clinical settings and meet the sharply increasing demand for POC tests. This review aims to provide an overview of the progression of multiplexed immunosensing techniques (focusing on spatial, time division, frequency division, barcoded, and particle based multiplexing), unveil the challenges each technique faces, and summarise the promising laboratory-based strategies under the development and how to translate them into clinical settings. We also briefly review multiplexed POC immunosensor areas that have recently gained increasing interest for clinical diagnostics. In the end, we share our vision for future trends in multiplexed immunosensors development for the diagnosis of progressive diseases.

2. Strategies for multiplexed biosensing

Over the past decade, multiplexed sensing platforms have been widely reported, as summarised in Table 1. The strategies can be categorised into spatial multiplexing, time division multiplexing, frequency division multiplexing, barcode multiplexing, and particle based multiplexing. The main transducers employed in multiplexed biosensing, to convert the energy from the biorecognition process into a readable signal, involve electrical, electrochemical, and optical methods.

2.1. Spatial multiplexing

Spatial multiplexing has been one of most widely reported multiplexing strategies, as this configuration allows for the minimisation of detection interferences and is compatible with most measurement methods. For electrical measurements, the sensing mechanism is commonly based on field-effect transistors (FETs). Each individual transistor consists of a conductive/semiconductive channel that is modified with a specific antibody. Upon binding of the corresponding antigen on the sensing channel, the drain-source current can be modulated, from which the concentration of the target biomarker can be determined (Li et al., 2019). The representative configuration of a spatial electrical sensor array consists of sensors located at different spatial positions, and each sensor may consist of several electrodes for the quantification of one specific biomarker. An example of early milestone work in this area comes from Zheng et al. who developed an electrical multiplexed sensor for the detection of cancer biomarkers using silicon nanowires (Zheng et al., 2005). These sensors used FET configuration, and each chip consisted of 200 individual and electrically addressable sensors, as shown in Fig. 3 (a). The high specificity for the simultaneous detection of three cancer biomarkers was achieved by immobilising the corresponding antibodies on different sensors. More recently, Kim et al. reported a carbon nanotube (CNT)-based multiplexed electrical immunosensor for the simultaneous detection of Alzheimer's disease biomarkers amyloid beta (Aβ) 40, Aβ42, phosphorylated tau (p-tau), and total tau (t-tau) with negligible crosstalk (Kim et al., 2020). The sensor employed densely aligned CNTs as transducing materials, and sensor arrays were functionalised with corresponding antibodies for Aβ40, Aβ42, p-tau, and t-tau respectively, as shown in Fig. 3 (b). Since the highly aligned CNTs in sensing channels reduced the density of tube-to-tube junctions and ensures a constant number of CNTs for each sensor, it showed record high sensitivities of 2.20 fM, 2.13 fM, 2.72 fM, and 2.45 fM for the proposed biomarkers in the same clinical samples.

For electrochemical immunosensors, detection can be achieved through monitoring either the change of surface electrochemical conductivity or the concentration of an electroactive substances directly associated with the antigen or antibody (Mahato et al., 2018). The former mechanism relies on the binding of the antigen onto the sensor surface modified with the corresponding antibody, changing the
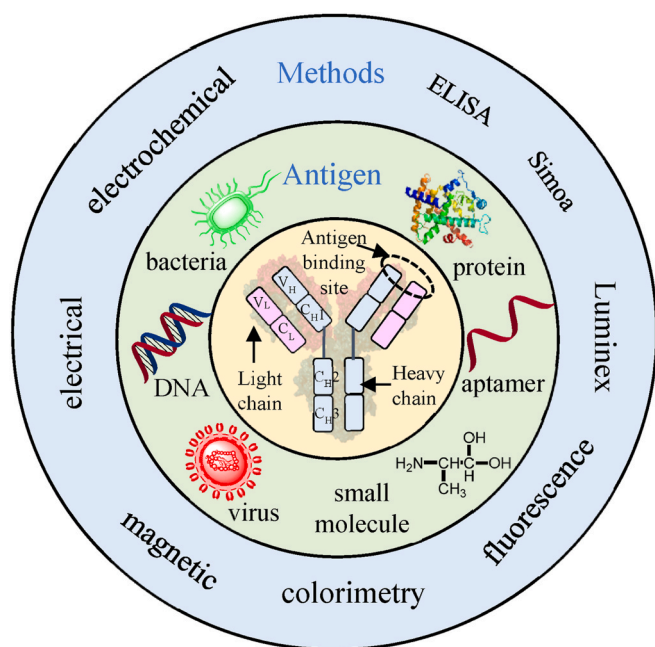

Fig. 1. The molecular structure of an antibody (yellow circle), its applications in immunosensing of various analytes (green circle), and the corresponding measurement methods (blue circle).
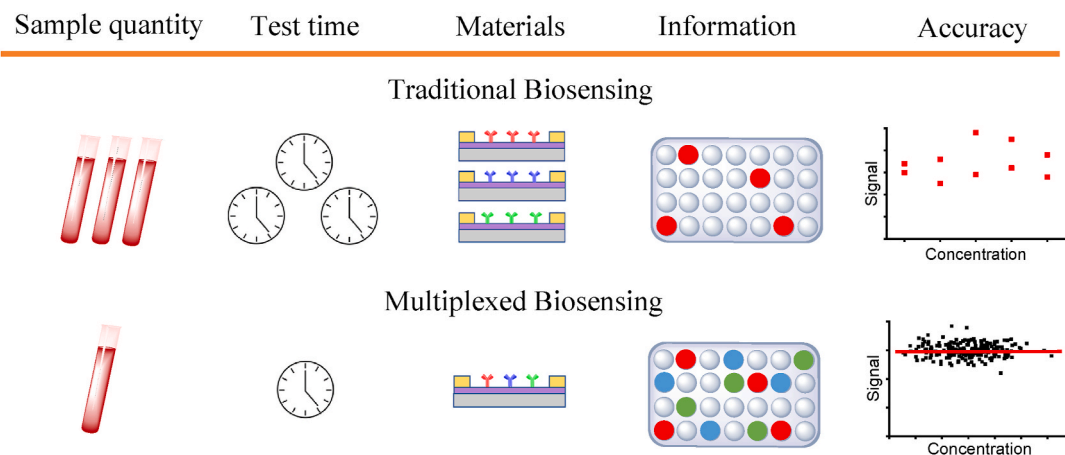
Fig. 2. Advantages of multiplexed immunosensors include less sample consumption, less averaged test time and materials for individual biomarkers, more informative detection results, and more statistically reliable conclusions.

Table 1

Examples of multiplexed immunosensors categorised according to multiplexing strategies, type of platform, overall size, number of sensor units, and performance.

Strategy	Type of platform	Size (mm)	Sensor Units	LOD	Ref
Spatial	Silicon-nanowire FET	8 × 1.2	200	2 fM (PSA), 0.55 fM (CEA), 0.49 fM (mucin-1)	Zheng et al. (2005)
Spatial	Optical CMOS-based imager	45 × 20	3	300 CFU[a]/ml (*C. trachomatis*), 1500 CFU/ml (*N. gonorrhoeae*)	Soler et al. (2017)
Spatial	Lateral flow calorimetric device	10 × 2.5	3	21.5 μg/mL alpha-defensin, 8.3 μg/mL (CRP[b])	Tsai et al. (2019)
Spatial	Carbon nanotube-based sensor array	–	4	2.20 fM (Aβ40), 2.13 fM (Aβ42), 2.72 fM (p-tau), 2.45 fM (t-tau)	Kim et al. (2020)
Spatial	Electrochemical array (WE, CE and RE)	7 × 2.5	4	24.7 pg/mL (PCT), 0.9 ng/mL (CRP), 5.1 ng/mL (PAMPs[c])	Zupančič et al., 2021
Time division	Potentiostat and on-chip amperometry paper array	–	8	0.35 mM (glucose), 1.76 (lactate), 0.52 mM (uric acid)	Zhao et al. (2013)
Time division	Chemi-impedance sensor array	13 × 4	4	7.58% operation variability (Cortisol) at pH 4 -8	Sankhala et al. (2018)
Time division	Amperometry sensor array	–	16	5.0 pg/mL (IL-6), 38 pg/mL (PCT)	Wu et al. (2018)
Time division	Light addressable potentiometric sensor system	10 × 10	4	6–8 x 10^{-6} mol/L (Na^{2+}), 5–6 x 10^{-6} mol/L (K^{+}), 4 × 10^{-6} mol/L (Ca^{2+}) and $<10^{-9}$ mol/L (H^{+})	Liang et al. (2021)
Time division	Dual EIS and SERS detection system	–	2	0.25 ng/mL (EIS), 0.025 ng/mL (SERS) for carcinoembryonic antigen	Castaño-Guerrero et al. (2021)
Frequency division	Frequency-tunable nanoshearing force microfluidics	40 × 15	100	Fast (≈5 min) naked-eye colorimetric detection of HER2, PSA and IgG.	Vaidyanathan et al. (2015)
Frequency division	Impedance spectroscopy multi-marker platform	–	2	Co-immobilised frequencies of 175.8 Hz (LDL) and 5.49 Hz (HDL)	Lin et al. (2017)
Frequency division	GMR biosensor array	4 × 2.5	12	MNPs at signal level as low as 6.92 ppm	Kim et al. (2018)
Frequency division	GMR immunosensor	–	40	0.52 ng/mL (AFP), 0.27 ng/mL (CEA), 0.5 ng/mL (NSE[d]), 0.3 ng/mL (SCC[e])	Gao et al. (2019)
Barcoded	Node-pore sensing with resistive-pulse sensors	0.01 × 0.5	4	$V_{particle}/V_{pore} \geq 1.2 \times 10^{-9}$ Virus size range: 100–200 nm	Balakrishnan et al. (2015)
Barcoded	Codabar paper-based assay	300 × 80	8	8 ng/mL (ENF[f])	Yang et al. (2017)
Barcoded	Impedance microfluidic digital barcoded array	1 × 0.1	2	6.5 μm (blood cells microsphere diameter)	Prakash et al. (2020)
Barcoded	Colorimetric lateral flow immunosensor	70 × 45	2	False negative rate of 40.0% (10/25) for SARS-CoV-2 IgA in serum	Roda et al. (2021)
Particle based	Electrochemical immunoassay with composite aggregation	20 × 15	2	0.650 pg/mL (CEA), 0.885 pg/mL (AFP)	Jia et al. (2014)
Particle based	Miniaturised flow chronoamperometry detection array	44 × 25	12	4 pg/mL cardiovascular biomarker	Moral-Vico et al. (2015)
Particle based	rGO immunosensor assay	–	3	91 fg/mL (CEA), 101 fg/mL (PSA), 83 fg/mL (AFP)	Zhao et al. (2019)

[a] CFU: colony forming units.
[b] CRP: C-reactive protein.
[c] PAMPs: pathogen-associated molecular proteins.
[d] NSE: neuron-specific enolase.
[e] SCC: squamous cell carcinoma antigen.
[f] ENF: enrofloxacin.

electrochemical impedance of the sensor; this change is directly proportional to the concentration of antigen bonded. This method suffers of poor specificity when applied in complex matrices as electrode surface conductivity can be affected by unspecific adsorption of sample species (Contreras-Naranjo and Aguilar, 2019). To improve its performance, this method normally includes an electroactive probe (e.g., potassium ferri/ferrocyanide) to evaluate the surface accessibility before and after the immunorecognition process (Khetani et al., 2018). The latter
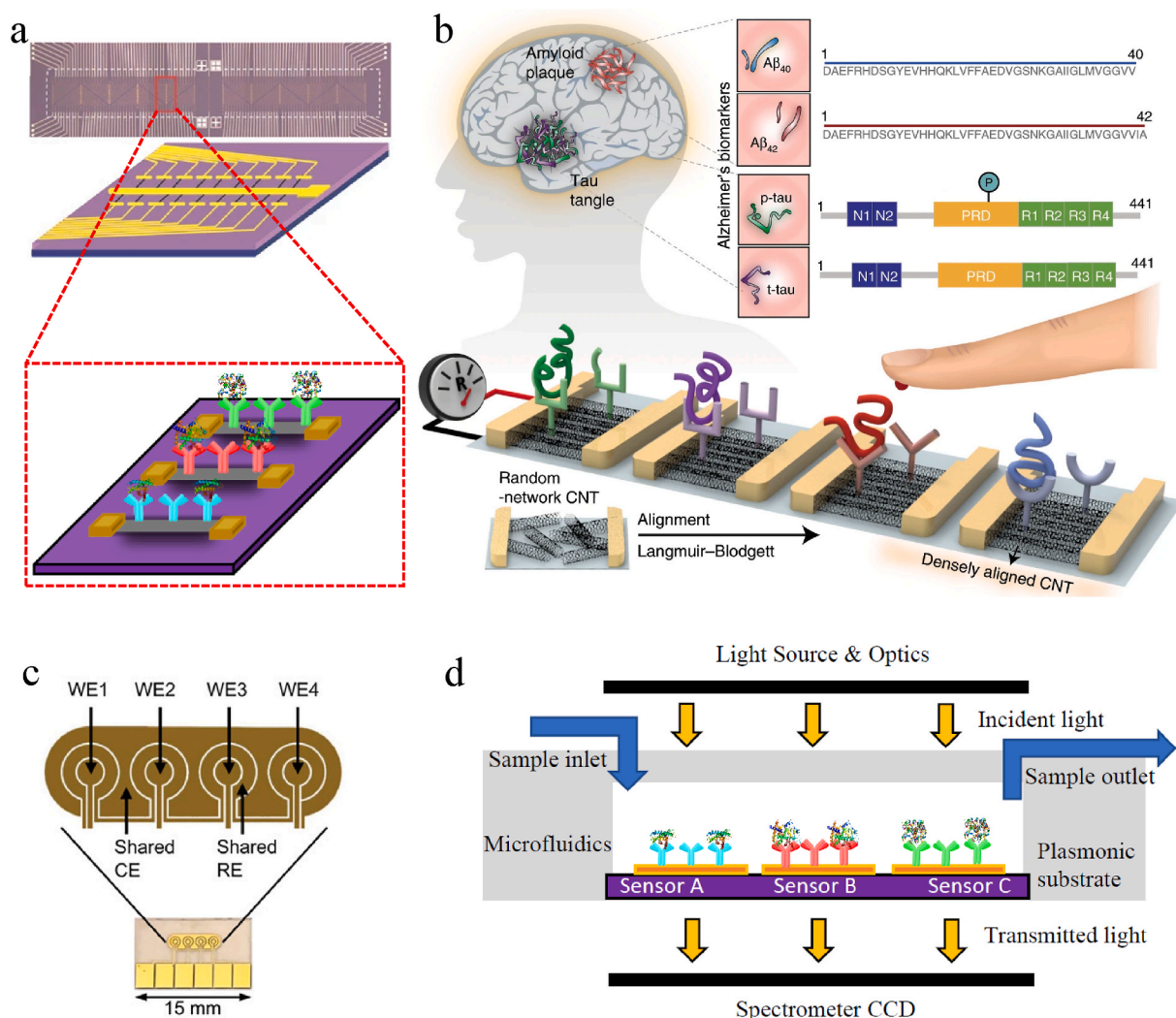
Fig. 3. Spatial multiplexed immunosensors. (a) A design of multiplexed FET sensors for the detection of cancer biomarkers using silicon nanowires. Reprinted with modifications by permission from Springer Nature Customer Service Centre GmbH: Springer Nature, Nat. Biotechnol., (Zheng et al., 2005), Copyright 2005. (b) The CNT-based FET immunosensor for the simultaneous detection of Aβ40, Aβ42, p-tau, and t-tau. Reprinted by permission from Creative Commons CC BY License: Springer Nature, Nat. Commun., (Kim et al., 2020), Copyright 2020. Each sensor array consists of an individual sensor functionalised with one corresponding antibody. (c) Planar electrochemical sensor consists of four individual WEs, common CE, and quasi RE within 7 × 2.5 mm. Reprinted by permission from Creative Commons Attribute CC BY License: John Wiley and Sons, Adv. Funct. Mater., (Zupančič et al., 2021), Copyright 2021. (d) Plasmonic sensor array modified with different antibodies. Each microfluidic channel consists of 3 in-line sensor arrays with two specific sensors and one negative control. Reprinted with modifications from Biosens. Bioelectron., 94, (Soler et al., 2017), Copyright (2017), with permission from Elsevier.

mechanism is essentially measuring electroactive species within (Li et al., 2021) or associated to the captured antigens (Khetani et al., 2018). The configuration normally consists of a common reference electrode (RE), a common counter electrode (CE), and a spatially separated working electrode (WE) array (Wilson and Nie, 2006a; Zupančič et al., 2021). Each WE can be individually functionalised for the detection of different biomarkers, whilst the distances between working-reference and working-counter electrodes should be kept constant to ensure the reproducibility of the measurements. As one recent example, an electrochemical sensor, with four gold WEs that shared a pseudo reference gold electrode and CE, has been assembled in an area less than 7 × 2.5 mm, as shown in Fig. 3 (c) (Zupančič et al., 2021); such a design enabled the simultaneous detection of three different sepsis biomarkers. Due to the large spatial separation between each WE, diffusional interference can be eliminated to enhance the precision and accuracy of the sensing arrays.

Optical immunosensors are another major type of spatial immunosensors. Most of the current commercial immunoassays in laboratories use optical spatial readout strategies, such as the standard ELISA and the state-of-the-art Simoa technology, but none of these platforms meet the specific requirements for POC testing (mainly the requirement of a portable test reader for POC testing). To meet such a need, efforts have been put into the development of miniaturised SPR-based spatial immunosensors. One representative platform employs a SPR chip, which is composed of independent nanohole arrays, fabricated on silicon nitride substrates, and selectively functionalised with specific antibodies for the detection of two bacterial strains without cell lysis or DNA extraction, as shown in Fig. 3 (d) (Soler et al., 2017). Such a platform uses extraordinary optical transmission, which is achieved by normal light incidence and is compatible with light emitting diodes (LEDs) and complementary metal oxide semiconductor (CMOS)-based imagers. This allows extreme miniaturization of the device and represents a further step forward for rapid, point-of-care diagnosis. In addition to surface plasmonic sensors, other multiplexed optical immunosensors have been developed in parallel, including electro-chemiluminescent sensors (Kadimisetty et al., 2018), chemiluminescence sensors (Xianyu et al., 2018), and surface-enhanced Raman scattering (Banaei et al., 2017), which all present promising sensing performance in simultaneous

detection of multiple biomarkers. Most of these optical immunosensors, including the commercial systems, still require demanding laser excitation and optical signal capturing instrumentation. This makes their use in frontline clinical settings more complicated than electrical-based platforms. One exceptional example is lateral flow multiplexed colorimetric developed by Tsai et al., (2019), where detection can be simply achieved with naked eyes.

The spatial multiplexed biosensor is essentially a repeated array of one individual sensing unit, therefore, its sensitivity, limit-of-detection and signal to noise ratio are identical across the different units. This empowers the spatial multiplexed immunosensor with intrinsic advantages, such as the elimination of crosstalk interference without the requirement of complex structures or layout designs, as well as the ease of improving detection throughput (multiple analytes). Its disadvantages are also obvious, such as the challenge of integrating large numbers of sensor units, which requires a separate signal acquisition for each sensor; and the amount of time required for generating and processing the large amounts of sensing data. By combining the signals from multiple sensors into one waveform using signal multiplexing strategies, the sensor scalability can be improved with reduced data size and data processing time.

2.2. Time division multiplexing

Time division multiplexing involves combining the multiple signals originated from a sensor array or module into a single (extended) temporal signal. As opposed to spatial multiplexing, each sensor signal is acquired in fixed temporal segments and then overlapped together in the time domain with the other signals. Separation of individual sensor signals from the final combined signal is performed by identifying the respective temporal segment. So, instead of requiring multiple-channel acquisition systems as the parallel topology shown in Fig. 4 (a) (Molderez et al., 2021), time division multiplexing can be achieved with a single electronic channel that incorporates an analogue multiplexer where signals from different sensors are routed to the common acquisition channel. Advantages of this approach include a reduced array area devoted to the acquisition of the individual signals of different channels that can be best used to effectively increase the number of sensing elements, high-throughput, negligible crosstalk between elements and reduction of system complexity and generated data in comparison to spatial multiplexing. However, typical commercial off-the-shelf signal multiplexers have poorer input impedance characteristics than the analogue front-end of acquisition systems which can lead to the degradation of the output signal produced by the sensor itself (e.g., reduced signal-to-noise ratio). This is particularly serious in the case of large
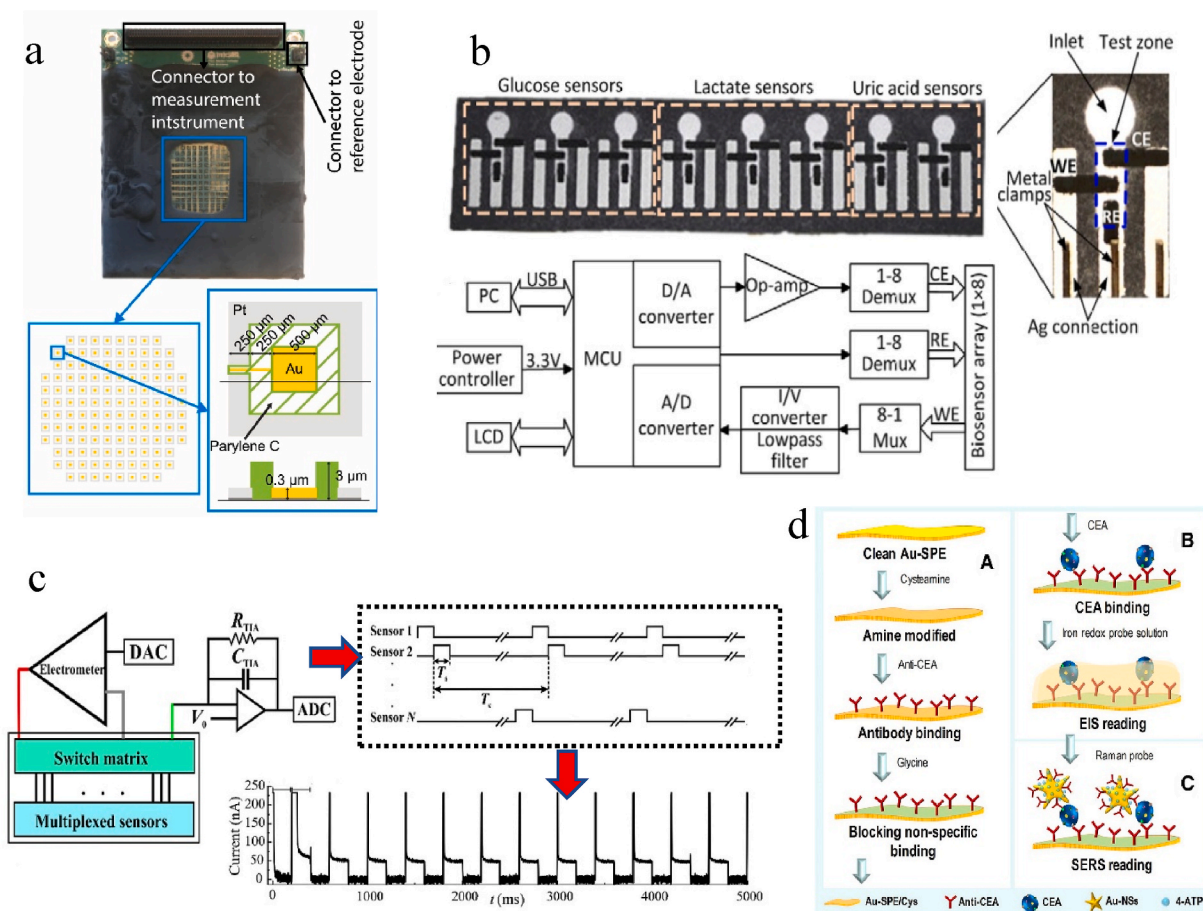

Fig. 4. Time division multiplexing. (a) High-throughput electrochemical system for anodic biofilms composed by 128 gold WEs and a common platinum CE. Reprinted from Biosens. Bioelectron., 174, (Molderez et al., 2021), Copyright (2021), with permission from Elsevier. (b) Microfluidic paper-based electrochemical biosensor that interfaces a multiplexed potentiostat architecture with 8 measurement channels (schematic) for detection of metabolic biomarkers. Reprinted by permission of the Creative Commons Attribution-NonCommercial-ShareAlike 3.0 License: National Institute for Materials Science, Sci. Technol. Adv. Mat., (Zhao et al., 2013), Copyright 2013. (c) Multiplexed amperometry system (schematic) with sequential switching sequence to measure each sensor and combination into a single current readout signal. Reprinted from Biosens. Bioelectron., 117, (Wu et al., 2018), Copyright (2018), with permission from Elsevier. (d) Sequential assembly of the CEA immunosensor with electrochemical (EIS) and SERS readings. Reprinted from Electrochim. Acta, 366, (Castaño-Guerrero et al., 2021), Copyright (2021), with permission from Elsevier.

impedance mismatch between the source signal (sensor) and multiplexing electronics, also hampered by the on-conduction resistance inside the multiplexer and stray capacitances, which are not negligible in many cases.

On the other hand, the sampling rate for data acquisition must increase to provide equivalent temporal segments for all the routed sensor channels and avoid anti-aliasing effects (Nyquist criteria). In general, the sampling rate must increase by a factor of *N* (number of channels) in order to keep the original (non-multiplexed) sampling rate. As time division multiplexing does not allow simultaneous signal acquisition for all channels in parallel, it is therefore limited to applications with low dynamic range for alternating current (AC) signals (spectral bandwidth), and unsuitable to detect fast transient events. Since chemical processes and reactions are usually very extensive in time, combined with acceptable signal levels produced by the different sensors within the array, time division offers a cheap yet reliable solution for multiplexed immunosensors provided that the switching process among sensors does not disturb the electrochemical reactions in progress (Liu et al., 2018c). Due to the simple electronic circuitry involved in time division multiplexing, several devices have already been shown in the literature during the last decade. For example, paper-based electrochemical arrays with different numbers of multiplexed immunosensors for detection and quantification of cancer biomarkers (Ge et al., 2012b) or other physiologically relevant metabolic biomarkers (Zhao et al., 2013), interfaced by a common potentiostat (acquisition system) or on-chip amperometry multiplexed systems (Fig. 4 (b)) for detection of enzymes with functionalised and addressable WEs in a timely manner (Jichun et al., 2005; Yang et al., 2009). More recent advances in time division multiplexing have led to the development of sensor arrays on flexible substrates, novel methodologies for sequential addressing individual sensors (architecture), multiplexed sensor activation and combinations of different biomarker detection techniques on the same sensing surface by precise timing control.

Sankhala et al. developed a flexible 4-channel chemi-impedance sensor fabricated on polyamide substrate with gold electrodes deposited by e-beam cryo-evaporation (Sankhala et al., 2018). These sensors targeted the measurement of cortisol in ultra-low volumes (1–3 μL) of perspired human sweat samples affected by local variations of pH (4–8) and temperature (25 - 40 °C). The gold surface of the sensors was functionalised with the dithiobis (succinimidyl propionate) linker by way of a 2-h incubation, followed by phosphate-buffered saline (PBS) wash-up and incubation again for 15 min with α-cortisol antibody prior to measurement. EIS measurements were performed by applying 10 mV of AC voltage (1 kHz) to each sensor in a combinatorial sequence with fixed measurement time (13 ms); applied voltage is controlled by a switch matrix inside a system-on-chip equipped with a discrete Fourier transform (DFT)-based impedance analyser. The DFT-based time division multiplexed sensor module proposed by Sankhala et al. takes advantage of the intrinsic impedance changes in response to cortisol-electrode binding. In this, the sensor can achieve stability of operation, with a level of 7.58% variability, under physiological pH and temperature changes; a relevant performance since the far-reaching systemic effects of cortisol in the body help to assure homeostasis. Following this, Wu et al. proposed a sequential multiplexing methodology for detection of human interleukin-6 (IL-6) and procalcitonin (PCT) by means of 5-fold multiplexed biosensors in an amperometry topology with WE and CE fabricated by deposition of titanium and gold onto a Pyrex wafer, whereas Ag/AgCl ink was used to build the REs (Wu et al., 2018). The authors also investigated different strategies to interface the single-chip potentiostat via single-pole/single-throw switches, with measurements alternating in time across the sensors as shown in Fig. 4 (c). Single-pole/single-throw switches were sufficient to capture the slow dynamics of the generated current profiles over the WEs caused by the higher concentration of beads carrying IL-6 or PCT (LODs estimated at 5.0 pg/mL and 38 pg/mL, respectively) and without causing significant signal artifacts produced by electrochemical reactions from

switching between sensors.

In a different approach, Liang et al. developed a light addressable potentiometric sensor system (ISLAPS) involved in physiological multiparameter detection through ion-sensitive membranes using silicone-rubber as the supporting material (Liang et al., 2021). The four detected sites for the sensors (Na^+, Ca^{2+}, K^+ and H^+) were automatically illuminated in sequence while detecting potentiometrically through a single hardware channel, thus obtaining a program-controlled time division multiplexing ISLAPS system for detection of ions in a single measurement frame lasting 1 min. Achieved LODs were on average 6–8 x10^{-6} mol/L, 5–6 x 10^{-6} mol/L, 4×10^{-6} mol/L and $<10^{-9}$ mol/L for the Na^+, K^+, Ca^{2+} and H^+ ions, respectively. This shows sensitivities comparable to previously reported field-effect ion-sensing but requiring smaller sample volumes and achieving long-term signal stability for more than 3 months. Castano-Guerrero et al. proposed an innovative dual detection approach for carcinoembryonic antigen (CEA), combining EIS measurements and SERS in sequential time readings over the same sensing layer (Castaño-Guerrero et al., 2021). This was achieved by establishing an antibody binding stage (first incubation) on modified screen-printed electrodes to yield EIS measurements (frequency step of 10 Hz and 2.5 mV amplitude), followed by a second antibody binding stage on the same layer using gold nanostars and a Raman probe for SERS, as depicted in Fig. 4 (d). The proposed device showed a linear response range of CEA from 0.25 to 250 ng/mL in EIS, whereas SERS spectra confirmed CEA detection within 0.025–250 ng/mL. Overall, this study pioneered the combination of EIS and SERS methods for immunosensors through sequential readings on the same sensing layer, increasing the accuracy of the detected data. The proposed method is also simple to implement and adaptable to new multiplexing devices by the coordination of incubation and measurement stages.

2.3. Frequency division multiplexing

In frequency division multiplexing, the signals originating from each sensor in a multiplexed device/array are combined in the frequency domain to generate a single signal, dramatically reducing the amount of measured data and complexity of the electronic readout circuitry. Original individual signals can then be recovered afterwards in the digital or computational domain by frequency demultiplexing techniques such as Fast Fourier transform (or its derivatives) and band pass filtering. The encoding frequency signals applied to each sensor can be imposed externally to the device by means of signal generators (as in the case of EIS measurements), or internally through selective modification of the geometry of the measurement electrodes or associated fluidic channels on the sensing substrate. The use of external signal generators requires complex signal processing techniques to decode the individual frequency-carrying signals but simpler measurement equipment than internal approaches. Internal methods to ensure frequency division multiplexing, however, require advanced microfabrication techniques to tailor the geometry of the sensing substrate or units for the correct generation of the encoding frequency patterns, thus, proving exceedingly difficult to apply to nanopores and nanochannels biosensing (Liu et al., 2018c). Engineering electrode geometry has been achieved previously for simultaneous detection of three individual microfluidic channels in a frequency-multiplexing impedance sensor to measure the resistance of PBS solutions (Meissner et al., 2012). Due to differences in geometry, each microfluidic channel (or sub-segment of the sensor) exhibited different double layer capacitance, which could be modelled into three RC circuits without signal overlap due to the unique specific peak resistance frequency (PRF) response of each sub-segment. Other multiplexed frequency encoding schemes used the node pore sensing (NPS) approach generated by the passage of cells through pores with different spacing between them (Balakrishnan et al., 2013), allowing accurate measurement of particle/cell sizes with increased spectral dynamic range. In this case, little external equipment in the form of AC

signal generators or data acquisition systems were required as the encoding frequencies are generated by the channel geometry and flow rates, given that the latter parameter is precisely controlled.

However, most of the frequency division multiplexing approaches found in the literature still rely on some sort of external AC signal generation. This has been used to detect cells by simultaneously measuring the resistive pulses produced on electrodes by the passage of said cells through parallel microfluidic channels (Coulter devices), thus achieving high-throughput detection (Jagtiani et al., 2011), an exception relative to the EIS-based multiplexing approach commonly in use these days. The EIS measurements originated from multiple sensors can

be multiplexed into a combined signal if each individual sensor is measured at a specific frequency or possesses an optimal (characteristic) frequency response. The optimal frequency of a biomarker in the AC stimulation regime is intrinsically related to the frequency at which the resulting impedance best represents the electric interaction between the biomarker and the recognition element on the sensing substrate. Advantages include label-free detection ability, improved sensitivity relative to other electrochemical measurement methods and speed of detection for a single biomarker (concentration). While it does not pose a great challenge in single biomarker detection, the burden of simultaneous detection of multiple biomarkers (and other noise sources) on a
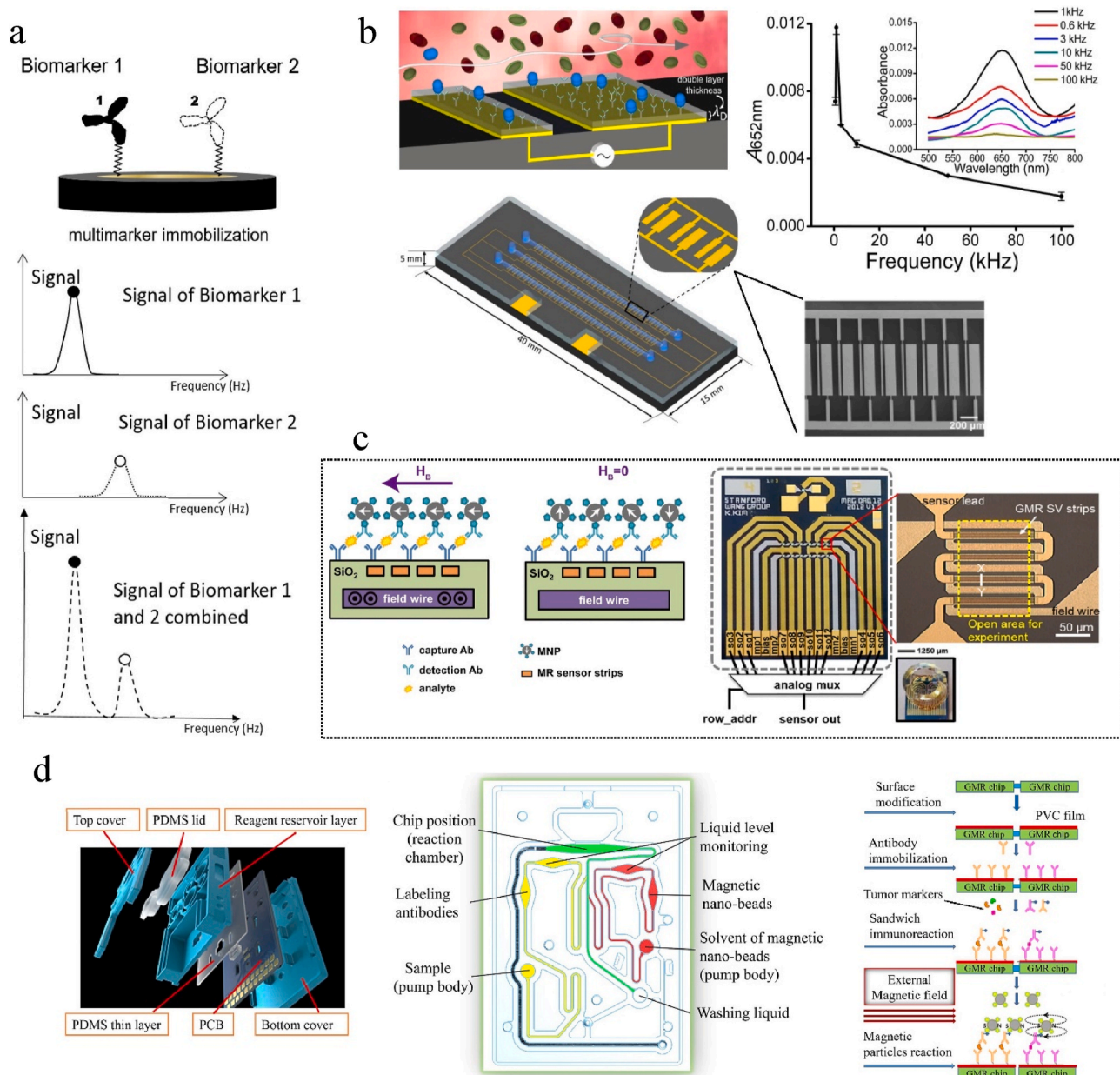

Fig. 5. Frequency division multiplexing. (a) Schematic representation of two biomarkers' immobilisation on the same substrate, with respective individual imaginary impedances recorded, followed by signal overlap with discernible optimal frequencies detection method. Reprinted from Biosens. Bioelectron., 89, (Lin et al., 2017), Copyright (2017), with permission from Elsevier. (b) AC-EHD induced nanoshearing across an electrode pair (schematic) employed for multiplexed microfluidic protein biomarker detection with 3 independent channels and graphical effect on frequency from protein capture. Reprinted by permission from Creative Commons CC BY License: Springer Nature, Sci. Rep., (Vaidyanathan et al., 2015), Copyright 2015. (c) Magnetic correlated double sampling technique with giant magnetoresistance (GMR) biosensor for antibody detection in a sandwich structure tethering magnetic nanoparticles (MNPs) to the surface (diagram) and photograph of the proposed biochip. Reprinted by permission from Creative Commons CC BY License: Springer Nature, Sci. Rep., (Kim et al., 2018), Copyright 2018. (d) Multilayer structure of the test card for tumour multi-biomarker immunoassay biosensor with GMR chip mounted on a PCB (left) and microchannel system (right). Reprinted from Biosens. Bioelectron., 123, (Gao et al., 2019), Copyright (2019), with permission from Elsevier.

single device can incur issues such as signal overlap and similar spectral harmonics, in combination with the electronic requirement of sweeping through a wide range of AC frequencies (10° Hz to 10^3 kHz).

With this in mind, Lin et al. employed EIS to detect the optimal frequencies of purified low- and high-density lipoproteins (LDL and HDL) co-immobilised on a multi-marked platform (Lin et al., 2017). The electrochemical responses of LDL and HDL were first individually characterised through the immobilisation of their recognition elements (MREs) onto gold CEs. AC measurements were taken using 5 mV amplitude sine waves with frequency sweeping from 1 Hz to 100 kHz. Then, co-immobilisation of both analytes was performed in the same conditions, as shown in Fig. 5 (a). The authors reported optimal frequencies of 81.28 Hz and 5.49 Hz for LDL and HDL, respectively, that shifted to 175.8 Hz and 5.49 Hz after co-immobilisation on the same platform. With these results, the authors highlighted the importance of the uniqueness of the detected peaks and higher specificity obtained using the imaginary impedance component of the measured signal only, rather than the broader signal yielded by complex impedance, where the latter poses a great challenge in signal decoupling and back-calculation of target concentrations in multi-marker detection.

Finally, other relevant approaches rely on the use of external AC stimulation to tune the nano shearing forces for specific detection of multiple protein biomarkers in serum, and GMR sensors for tumour marker detection through magnetic nanoparticles and nano-beads attached to the surface of the chip array. Vaidyanathan et al. developed a multiplexed device composed of 100 asymmetric electrode pairs exhibited in Fig. 5 (b) and functionalised with capture antibodies specific to human epidermal growth factor receptor 2 (HER2), prostate specific antigens (PSA) and immunoglobulin (Vaidyanathan et al., 2015). Serum samples were afterwards passed through the device under the influence of an optimal AC-field, ranging from 600 Hz to 100 kHz ($V_{pp} = 100$ mV), simultaneously, and proteins were detected by colorimetric readouts (determined by colour change detectable by the naked eye). The results suggested that the variation on the capture levels with applied AC frequency was due to the manipulation of shear forces within the double layer of the functionalised electrodes (specific and nonspecific protein binding phenomena), thus yielding a means for frequency signal separation in multiplexed devices. Kim et al. developed a scalable GMR biosensor array with on-chip magnetic field generator and a high-speed acquisition method based on magnetic correlated double sampling to detect nanoparticles at a signal level as low as 6.92 ppm, thus bridging the gap between frequency division and particle-based multiplexing (Kim et al., 2018). The system includes a GMR sensor array with magnetic field generator strip line inductors embedded on the chip directly under the sensors that magnetises the magnetic particles, as shown in Fig. 5 (c). This induced a local magnetic field detectable by the sensors which, in turn resulted in extremely low, femto-Molar LOD. A low LOD is paramount as biological samples are rarely magnetic. Gao et al. went further to develop a GMR multi-biomarkers immunosensor to detect 12 tumour markers simultaneously, which comprised a GMR sensor array, a microfluidic device, and magnetic nano-bead labels over a double antibody sandwich immunoassay (Gao et al., 2019). The system exhibited in Fig. 5 (d) yielded a very competitive point-of-care testing platform by combining GMR and microfluidics technologies, achieving excellent sensitivity, accuracy, and stability with fast reading times.

2.4. Barcoded multiplexing

A barcode multiplexed immunosensor is a derivative of the spatial multiplexing platform, which measures target biomarkers or barcode labels in a programmable order. One type of barcode multiplexed immunosensor is integrated with microfluidic channels consisting of a few separated node-like sections: each section is functionalised with one specific antibody. The sensor is particularly useful for the detection of particles carrying multiple surface biomarkers, such as a cell. The sensing mechanism is: when a cell travels through the microfluidic channel, its surface biomarkers interacts with immobilised antibodies in the particular node-like sections, and therefore moves more slowly through this particular section than other sections, as shown in Fig. 6 (a) (Balakrishnan et al., 2015). This leads to a longer current pulse within the barcode-like output signal. By analysing the duration of these pulses to that of the control, the qualitative detection of surface biomarker can be achieved. This barcode-based electrical platform can identify and measure the percentage of particles carrying target biomarkers, and the number of biomarkers to be measured can be easily increased by adding additional sections with the potential of error calibration (Wang et al., 2021). However, this method detects the particles carrying surface biomarkers and therefore has a limited capability in detecting intracellular and free-standing biomarkers. Compared with spatial multiplexing, it also requires the biomarker-carrying particles to pass through all the barcodes without being captured/immobilised onto the sensor surface.

In addition to analysing the pulse duration, micro electrical barcodes have been produced as digital labels to generate programmable impedance signals under a radio frequency (RF) reader (Wood et al., 2007). To understand the working principle, each of these barcodes consists of aluminium stripes with different widths, which are sandwiched between SU-8 layers and functionalised with antibodies to bind with specific antigens. When the barcodes pass through the RF reader, the aluminium strip is read as "1" for per unit length and the space between aluminium strips is read as "0" for per unit length. When a particle carrying multiple biomarkers (multiple micro barcodes) passes through the reader, detection signals will be significantly overlapped; this could prove to be an obstacle for multiplexed biosensing. Although the technique has been further improved using multiple readout electrodes (Prakash et al., 2020) or orthogonally resistive pulse sensing from a single electrical output (Liu et al., 2016) (as shown in Fig. 6(b–c)) to address the issue of overlapped signal, its application is restricted to the detection of particle numbers and sizes, and its potential as an immunosensor platform needs to be further explored.

On the other hand, promising progress has been made for optical multiplexed immunosensors. One representative example is the multiplexed lateral flow assays (LFA), which could utilise optical signal generated by colorimetric (Xu et al., 2020), fluorescent (Jin et al., 2021), or chemiluminescent mechanisms (Roda et al., 2021). This Codabar-like configuration includes dark barcodes, white spaces, and invisible barcodes (printed on white spaces with specific capture antibodies) with different widths between each other to encode information (Yang et al., 2017), as shown in Fig. 6 (d). Upon the injection of sample solutions, all different biomarkers bind with their corresponding antibody, which are labelled with gold nanoparticles (AuNPs) and pre-stored in the conjugate pad. Then all labelled biomarkers pass through the barcode region in order, while the target biomarkers are captured by those invisible barcodes on specific areas. The change of colour in the invisible barcodes, leading to the change of the original barcode widths, shows the detection results of multiple biomarkers, as shown in Fig. 6 (d). Similar with standard LFA, the advantages of multiplexed LFA includes low cost, disposability, simple operation, and rapid detection, but inadequate LODs (nanogram per millilitre) limit their use for the detection of many biomarkers with clinical concentrations at picogram per millilitre level, such as most of the blood neurodegenerative biomarkers (Li et al., 2020).

2.5. Particle based multiplexing

Particle based multiplexing relies on the affinity of micro/nano particles to create beads, aggregates, or colloids for the detection of biomarkers. Due to their small size, many active sites for detection can be designed on the sensing substrate, whereas functionalisation with specific antigen/antibodies can lead to targeted multi-biomarker recognition (surface modification). Advantages include higher surface-to-volume ratios for detection, as more binding sites are available than
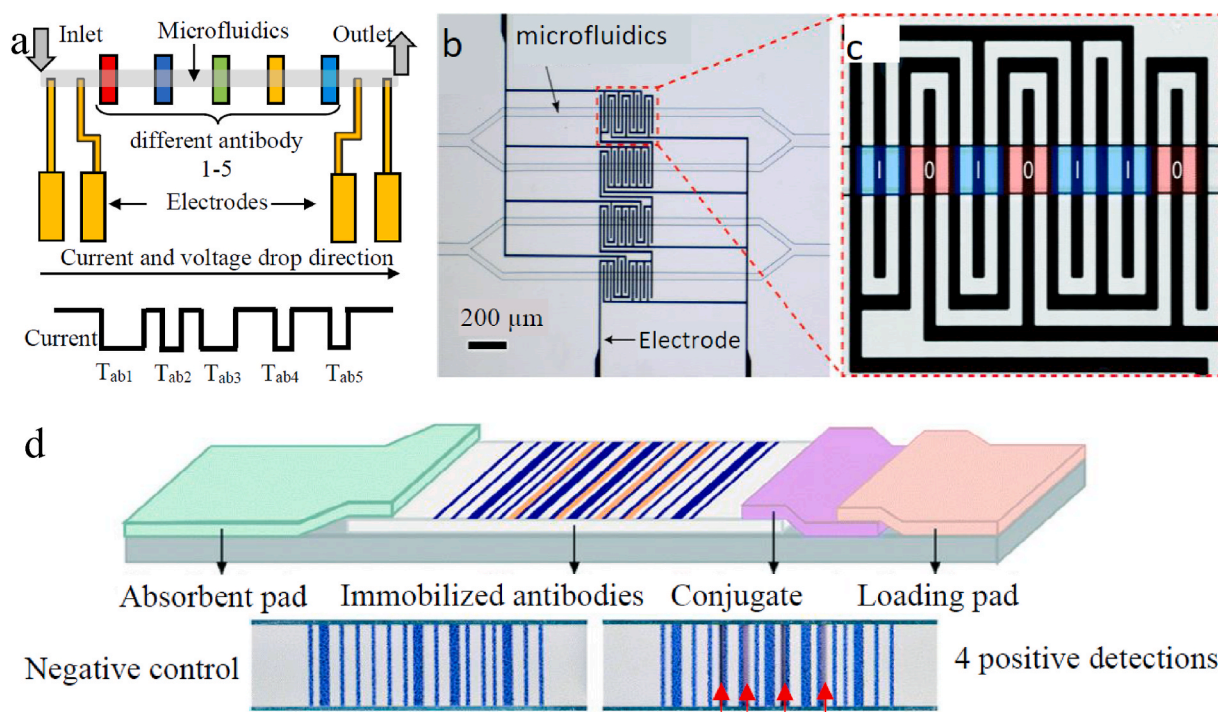
Fig. 6. Code multiplexed immunosensors. (a) Schematic of electrical barcode multiplexing sensor functionalised with different antibodies. When a biomarker-carrying particle travels through the microfluidic channel, the change of current pulse reflects the interactions between the biomarkers on the particle surface and the immobilised antibodies. (b) and (c) Design of orthogonal digital codes for the electrical detection of particles flowing through polydimethylsiloxane (PDMS) microfluidic channels. Reproduced from (Liu et al., 2016) with permission from the Royal Society of Chemistry. (d) Schematic of optical barcode multiplexed immunosensor (LFA). The Codabar-like region includes dark barcodes, white spaces, and invisible barcodes (specific capture antibodies). Upon the conjugation between capture antibody and AuNPs labelled biomarker, the dark barcodes change their widths and show the detection towards multiple biomarkers. Reproduced from (Yang et al., 2017) with permission from the Royal Society of Chemistry.

conventional electrodes; enhancement of electron transfer between species in the aggregation structure, further increased by the unique magnetic properties of some particles in the aggregate (higher specificity); and the size distribution of these particles can be specifically controlled to favour multiplexed multi-biomarker detection (Liu et al., 2018c). However, the particle based multiplexing has some disadvantages. For example, advanced micro/nano fabrication and functionalisation are required to produce the multiplexed sensing channels with different pore sizes. The complex sensor structure will lead to less reproducibility/stability and higher cost for POC use; the particles (especially metallic particles) are electrically unstable, which means they could aggregate in the presence of salts in biological environment. This non-specific attachment/aggregation will contribute to a decrease in the final output and detection issues for particle-based multiplexing. Therefore, dedicated sensor surface optimisation is needed when this method is used in clinical samples; the sensitivity and detection range achieved by using particles is inconsistent among literatures. Also, strict quality control for particle production and processing is needed to improve the reproducibility and the reliability of detections.

Nonetheless, this type of multiplexing has been used previously to detect human granulocyte colony stimulating factor, and granulocyte and macrophage colony stimulating factor on a single chip due to the increase in size of a colloid structure upon specific binding with an antibody. Then, nanopores were fabricated in the same microfluidic chip to separate the structures, with a low throughput level (Carbonaro and Sohn, 2005). It has been also used for the simultaneous detection of microparticles with different sizes and magnetic properties in immune-aggregation platforms (Han et al., 2016b), such as anti-rabbit IgG and human ferritin in various concentrations, with the latter being dotted with magnetic particles captured by the applied magnetic field before proceeding to a second micro-Coulter counter. Still, nonspecific attachment occurred leading to lower sensitivity and limits of detection,

which can be overcome by recruiting anti-fouling materials at the aggregation surface.

Jia et al. developed a label-free immunosensor for simultaneous detection of CEA and α-fetoprotein (AFP) using indium tin oxide (ITO) sheets for the WEs and graphene nanocomposites as the supporting matrix involved in antibody-antigen immunocomplex detection (Jia et al., 2014). To avoid the functionalisation of graphene through a harsh coupling reaction, the authors employed polyethyleneimine (PEI) functionalised reduced graphene oxide (rGO) for direct loading of thionine (Thi) and AuNPs to immobilise anti-CEA on ITO, whereas Prussian Blue (PB) and AuNPs were used to immobilise anti-AFP. A decrease in the electric current response of both Thi and PB was achieved by the formation of the antibody-antigen complex, proportional to the concentration of the corresponding antigen, yielding LODs of 0.650 pg/mL and 0.885 pg/mL for CEA and AFP, respectively, in the linear working range of 0.01–300 mg/mL. Wu et al. developed a microparticle (MP)-based immunoaggregation assay for detection of goat anti-rabbit IgG and human ferritin as model macromolecular biomarkers by inducing the formation of aggregation in PBS and 10% FBS solutions (Han et al., 2014; Wu et al., 2015). Antibodies (Ab) were firstly conjugated to MPs through streptavidin-biotin interaction, as shown in Fig. 7 (a). Then, the addition of the biomarkers caused aggregation of Ab-MPs. The aggregation could be detected by electrical particle counting devices, translating the invisible nanometre-scale of the biomarker into detectable changes in micrometre-scale particle size distributions. The authors found not only that the number and volume ratios of the aggregates were directly correlated to biomarker concentrations but also that the detection range could be tuned by adjusting the Ab-MPs concentration. By its turn, Moral-Vico et al. developed a miniaturised flow cell for multiplexed chronoamperometric detection of myeloperoxidase (MPO) using immunofunctionalised magnetic beads (MBs) under substrate flow and stopped-flow approaches (Moral-Vico et al., 2015), using
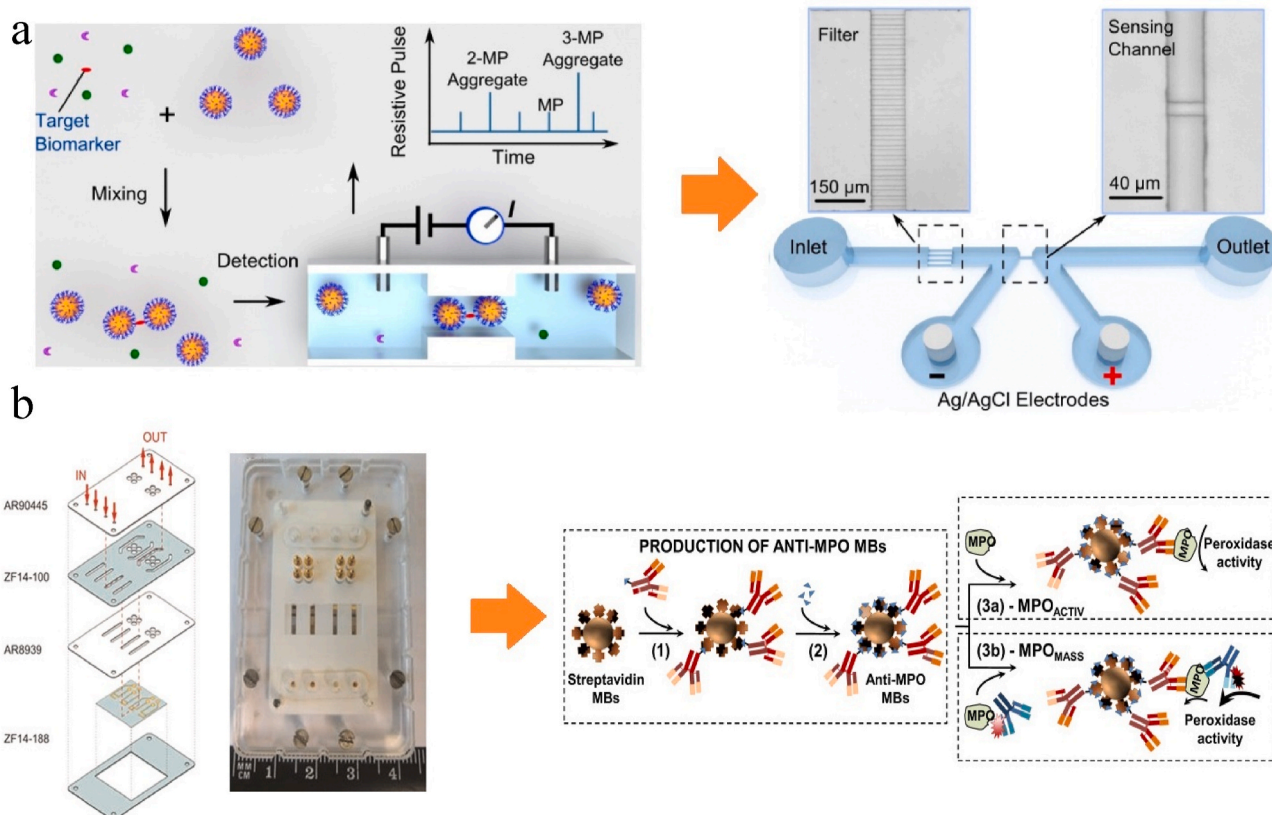
Fig. 7. Particle based multiplexing. (a) Biomarker assay mechanism based on immunoaggregation (left) with detection by a microfluidic resistive pulse sensor (right). Adapted with permission from (Han et al., 2014), Copyright 2014, American Chemical Society. (b) Images of the microfluidic chip device assembly (left) used for dual chronoamperometric detection of peroxidase activity with magnetic beads (MBs) and modified with anti-MPO (right). Reprinted from Biosens. Bioelectron., 69, (Moral-Vico et al., 2015), Copyright (2015), with permission from Elsevier.

a simple fabrication process (Fig. 7 (b)). This dual MPO mass and activity assay was applied to the study of 10 clinical plasma samples, with electrochemical measurements being carried out inside a Faraday's cage using a multi-potentiostat. The authors were able to achieve a LOD of 4 pg/mL using appropriate tuning of the detection and flow conditions, as well as the large immunocapture surface provided by MBs and incubation under magnetic rotation of the samples (i.e., enhancement of assay kinetics, shortening of incubation time, preconcentration of target biomarkers, and separation from other sample species). Liu et al. developed a high sensitivity microfluidic assay for detection of vascular endothelial growth factor (VEGF) using competitive immunoaggregation and continuous voltage pulse measurements with a micro-Coulter counter (Liu et al., 2018b). The detection principle was based on the competition of the targeted cell secretome protein VEGF and anti-biotin-coated microparticles for the specific binding with biotinylated antibodies, reducing the number of aggregates formed with functionalised MPs relative to VEGF-free samples. Therefore, a decrease in the average volume of functionalised MP aggregates gives an indication of cell secretome concentration. With this method, the authors were able to achieve a detection range for VEGF (0.01 ng/mL to 100 ng/mL) comparable to that of ELISA, though involving easier sample preparation and measurements. Finally, Zhao et al. built on the advances of rGO to produce a sandwich-type multiplexed immunosensor assay for detection of 3 tumour markers (CEA, PSA, and AFP), through the development of PEI-polydopamine (PDA)/rGO nanocomposites (Zhao et al., 2019). PDA/rGO as the sensing platform was simultaneously loaded with detection antibodies and large amounts of PEI to immobilise different signal labels, which greatly increased the loading of the capture antibodies, as well as enhancing the electrochemical response signals and dispersion in aqueous solution. Regarding the measurements, cyclic voltammetry and differential pulse voltammetry were carried out to measure the electrochemical response of the multiplexed immunosensor assay, achieving an excellent linear response in the range of 0.1–120 pg/mL.

As a summary of section 2, we provide Table 2 that compares the associated merits and limitations of each multiplexing strategy discussed in the manuscript.

3. POC platforms for multiplexed immunosensors

To date, most clinical immunoassays require long sample incubation/processing time, expensive test kits, an invasive acquisition process, demanding laser excitation and emission capture instrumentation, and experienced personnel to operate and maintain the diagnostic system. These reasons limit their accessibility and availability as frontline diagnostic tools, especially for patients in lower-income regions and countries (Hampel et al., 2018). To address such a need, POC immunosensors that combine high-performance biosensors and low-complexity signal processing systems have recently gained increasing interest for the development of cost-effective, reliable, and rapid diagnostic platforms in resource-limited clinical settings, such as general practitioner (GP) surgeries, pharmacies, and care homes (Sheridan, 2020). One practically useful POC multiplexed immunosensor should meet the criteria including: minimal invasive acquisition process and sample volume, maximal information extracted from detection, simple patient intervention or operation, rapid sample-to-results turnover time (<2 h), cost-effective and portable readout system, adequate long storage and shelf life and, most importantly, clinically relevant sensitivity and accuracy (Dincer et al., 2017). This section will guide the readers through the progression in the most commonly developed POC

Table 2
Merits and drawbacks for the five multiplexed biosensing strategies.

Multiplexing method	Merits	Drawbacks
Spatial	. Identical sensitivity, LOD and signal-to-noise ratio across all sensor units composing the array.	. Integration of large number of sensor units into smaller areas.
	. Elimination of crosstalk interferences by simple design layouts.	. Separate signal acquisition interfaces for each sensor unit.
	. Improved detection throughput (multiple analytes) without using complex design structures.	. Large processing times due to the amount of generated data.
	. Compatibility with most transduction mechanisms (electrical, optical, and electrochemical).	. Requirement of external instruments for signal excitation and acquisition.
Time division	. Reduced number of acquisition channels (system complexity), down to a single (common) channel.	. Poor electrical impedance characteristics for the resulting common multiplexed signal.
	. Low-cost fabrication process.	. Parasitic interferences from on-conduction resistance and stray capacitances.
	. Reduced array area occupied.	. Not allows simultaneous signal acquisition for all sensor units in parallel.
	. Increased number of sensor units per array area and signal throughput.	. Limited to applications with low dynamic ranges (bandwidth), unsuitable for fast transient detection.
	. Reduced crosstalk interferences between sensor units.	
Frequency division	. Label-free detection, improved sensitivity, fast detection times, higher specificity attained at the resonance peak (frequency).	. Complex signal processing techniques involved (Fast Fourier Transform, demodulation, and band-pass filtering).
	. Reduction in the amount of data generated from the array (frequency encoding of the output signals into one common signal).	. Advanced microfabrication techniques to design internal encoding schemes (pores, fluidic channels, electrodes).
	. Encoding frequencies imposed by either external equipment or, internally, by selective manipulation of the electrode geometry, fluidic channels, or pores.	. Correct geometry tuning of the encoding frequency patterns can be challenging to apply to nanopores and nanochannels biosensing.
	. Simultaneous signal acquisition for the different sensor units in parallel.	. Spectral overlap of the signals originated from multi-marker detection, their harmonics and external noise interferences that degrade performance.
	. Unique specific resistance peak or optimal frequency response for each sensor unit.	
Barcoded	. Useful for the detection of particles carrying multiple surface biomarkers.	. Detection signals can severely overlap.
	. Increased number of detectable biomarkers by simple addition of more channel selective sections.	. Restricted to the detection of particle numbers and sizes only.
	. Low-cost, disposable, simple operation, and rapid detection (comparable to LFA).	. Inadequate LODs for clinical concentrations at picogram per millimetre level.
	. Coupling of Codabar-like configurations with readout systems that detect changes in optical signal strength.	. Limited capability in detecting intracellular and free-standing biomarkers.
		. Capture and immobilisation onto undesired barcode areas and/or sensor surfaces.
Particle based	. Increased number of active sites for detection due to the small particle sizes.	. Advanced micro/nano fabrication and functionalisation techniques for array design.

Table 2 (*continued*)

Multiplexing method	Merits	Drawbacks
	. Higher surface-to-volume ratios for detection.	. Less reproducibility, stability, and reliability of detection for the created structures and assembly.
	. Higher achievable specificity and signal enhancement due to unique magnetic and electric phenomena occurring at the microscopic aggregation level.	. Higher cost for POC use.
		. Non-specific attachment/aggregation of particles leading to signal degradation.

platforms for multiplexed immunosensors (namely, paper based platforms, microarray based platforms, and microfluidic based lab-on-chip platforms), unveil their technical challenges, and outlook their potential in frontline clinical settings.

3.1. Paper based platform

LFAs are the most well-established paper based POC platforms (including nitrocellulose membranes, although it is not paper), due to their structural simplicity, fast detection, and low production cost (Li and Macdonald, 2016b). One early example is the commercial product Triage Cardiac Panel (Quidel formerly Alere) that integrates the advantages of LFA with a miniaturised laser fluorescence readout system and offers simultaneous detection of up to three biomarkers from plasma or whole blood samples within 20 min (Alghamdi et al., 2020). The sensing mechanism is similar to the standard LFA that has been discussed in Fig. 6, which benefits from power-free sample loading (driven by capillary forces) and expertise-free operation. In 2016, a binary coded multiplexed LFA was reported for its simultaneous detection of 7 antigens using a single LFA array (Li and Macdonald, 2016a). The paper based sensing channel was divided into 7 segments, which of them were functionalised with specific antibodies and able to present the colorimetric information as digital displays. Such a novel design allowed the simultaneous detection of theoretically up to 127 discrete analytes with readout-free setup (naked eye reading). In parallel, other paper based multiplexed LFAs platforms were explored, involving the strategies of multiple lines detection (Noguera et al., 2011), bi-directional detection (Hossain et al., 2012), or multi-directional detection (Peters et al., 2015). But these latter works remain as laboratory techniques with limited demonstrable impact in clinical settings.

Multiplexed LFAs normally rely on the generation of optical signals as outputs (Taranova et al., 2015), but some recent approaches have explored the use of electrochemical detection to improve test sensitivity (Ruan et al., 2021). For example, Mao's group reported a multiplex electrochemical immunosensor, which combined the advantage of low-cost and rapid detection from LFA and the high sensitivities from AuNP-assisted electrochemical measurements (Mao et al., 2008). The method takes the idea of basic LFA, which consists of two different-antibody functionalised strips on a cellulose substrate. After the antibodies capture their corresponding AuNP-labelled biomarkers, these two strips were cut off and the AuNPs were dissolved in HBr–Br$_2$ solution, where gold ions (III) can be easily detected by square-wave voltammetry. This method still suffers from key disadvantages of LFAs (e.g., low reproducibility of disposable strips, relatively high sample consumption, and the need of a control for each detection) with one additional drawback due to the separated detection.

As a significant breakthrough of the cellulose paper based immunosensors, microfluidics has been fast developed to complement the LFA (known as microfluidic paper based analytical devices or µPADs) (Lisowski and Zarzycki, 2013). This technology not only shows a high degree of multiplexing capability and improved sensing performance, but also enables sample manipulation functions, such as liquid mixing, splitting (Abadian et al., 2017), and biological sample filtration (Pollock

et al., 2012). For example, Ge et al. demonstrated 3D multiplexed µPADs for the electrochemiluminescence detection of four biomarkers (Ge et al., 2012a). This µPAD platform allows the liquid sample to flow in all directions, and potentially distribute one single sample into hundreds of sensing points, enabling more sensing devices to be integrated within a limited footprint (Martinez et al., 2008). In this work, all three electrodes (working, counter, and reference) were screen-printed on paper with pre-printed wax microfluidics as reservoirs, and the eight working electrodes were functionalised with four specific antibodies, as shown in Fig. 8 (a). Upon the addition of sample solution and $(Ru(bpy)_3^{2+})$-labelled signal antibodies, $(Ru(bpy)_3^{2+})$-tri-n-propylamine (TPA) electrochemiluminescence was used for the detection of all four tumour biomarkers. In contrast to standard LFAs, µPADs have not been widely commercialised for POC diagnostic applications yet; this could be due to the increased production cost, the increased complexity of the production mechanism (numerous steps), the inadequate (semiquantitative) sensitivity and reproducibility (due to the nature of fabric based substrate and its interaction with complex biological samples), and its operational complexity (e.g., liquid injection, instrument-free comparison between control and readings). Although efforts have been made to combine cell phones or portable scanners to improve the portability (Lim et al., 2019), µPADs, especially in relation to multiplexed immunosensing, need to be further developed.

3.2. Microarray based platform

Microarray based platforms essentially employ the spatial or particle based multiplexing strategy for the simultaneous detection of multiple biomarkers. As one of the most well-established and standard techniques in clinical diagnosis, the high throughput multiplexed microarray can be easily plotted onto microscope slides with a resolution down to subpicolitre per spot using inkjet printing. The signal readout (detection) can be achieved through the optical method discussed in section 2 (Chen et al., 2018), by means of a scanning charge-coupled device or CMOS camera to measure the intensities of the laser-induced fluorescence (Chandra et al., 2011) or chemiluminescence (Kadimisetty et al., 2015) from the (differently) labelled secondary antibodies (Fig. 9 (a)). One excellent product is the Simoa platform, which has been used as the gold standard method for quantifying low concentration biomarkers at laboratory settings. By digitally counting half a million microbeads, which are distributed in spatially separated wells (one bead per well) and are labelled with up to four different capture antibodies (and fluorescence labels), this multiplexed technology offers LODs in the range of 10 fg/mL level in clinical body fluid samples (Lee et al., 2020; Norman et al., 2020), as shown in Fig. 9 (b). Although most of the microarray based systems require bulky laser excitation and signal capture, a few

miniaturised systems have been reported. For example, Hedde et al. developed a 3D-printed cost-effective and portable platform that can be deployed into frontline clinical settings for the detection of blood antibodies against 67 antigens from 23 strains of 10 respiratory infectious viruses including SARS-CoV-2 (Hedde et al., 2020). The optical measurement can also be performed in a label-free manner using the SPR technique on metallic sensor surfaces. As a successful demonstration, an SPR-based antibody microarray with spot sizes from 200 to 750 µm was created to simultaneously detect β2-microglobulin and cystatin C at a concentration of 1 nM–300 nM (Lee et al., 2006). However, the complexity and cost of this method require further optimisation for it to be practically useful in diagnostic applications.

The microarray readout can also be achieved via electrochemical methods with individually addressable microelectrodes. The most straightforward configuration consists of an array of individual microelectrodes, and shared reference and counter electrodes (Cooper et al., 2010). Eissa et al. successfully demonstrated a microarray based immunosensor for the simultaneous detection of three immunodeficiency disorder biomarkers with LODs down to a few picograms per millilitre (Eissa et al., 2018), as shown in Fig. 9 (c). This is a comparable performance to the state-of-the-art Simoa technology. Simply by replacing the corresponding capture antibodies on the surface of working electrodes, this platform has also demonstrated its potential for the sensitive detection of coronavirus (Layqah and Eissa, 2019) and up to seven tumour biomarkers (Wilson and Nie, 2006b; Wu et al., 2007). The electrode materials in this method, such as graphene or AuNPs (Li et al. 2015, 2020), play an important role in increasing the sensitivity of the immunosensor. However, it is usual for such electrode materials to also increase the complexity of the sensor and reduce reproducibility. Therefore, the sensitivity and the complexity of the immunosensor must be balanced carefully.

Compared with paper based platforms, microarray based platforms ensure rapid and high-throughput detection of multiple biomarkers. The use of solid-state substrates and CMOS fabrication, instead of paper platforms and drop-coating, significantly increases the integration level of the multiplexed units and improves the reproducibility and sensitivity of detection. There are, however, a few challenges that need to be addressed before microarrays can be deployed as clinically useful POC platforms; these challenges include the relatively high consumption of sample volume, the complicated pre-treatment of substrates (e.g., sample plotting using an inkjet printer), bulky instrumentation (especially for optical detection methods), and lack of sample preparation functions (e.g., disruptors separation, target biomarker enrichment). More importantly, liquid samples on the sensor surface remain unguided and uncontrolled in terms of size, shape, flow direction, and crosstalk between different spots. These issues need to be addressed to further
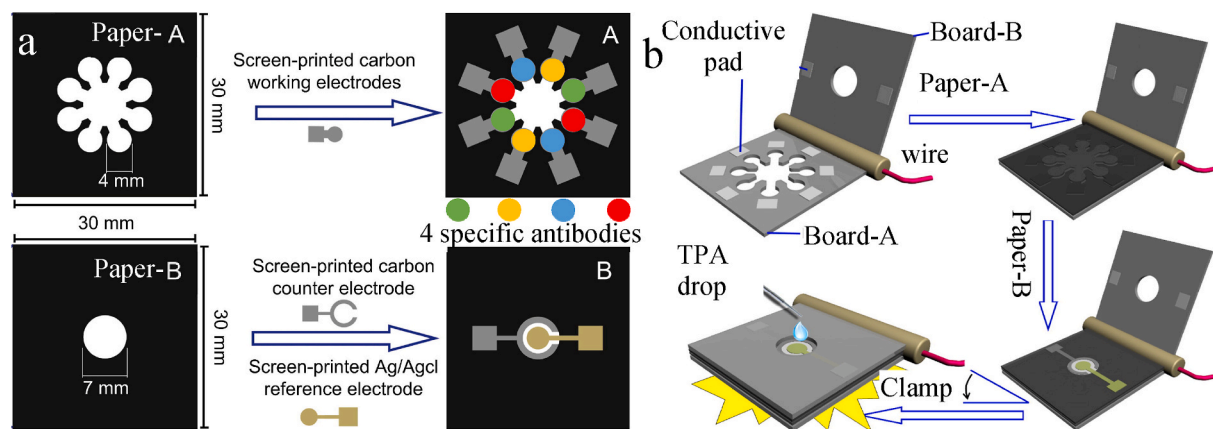

Fig. 8. Paper based multiplexed immunosensors. (a) 3D multiplexed µPADs for the electrochemiluminescence detection of four biomarkers. The microfluidics (as reservoirs) were firstly wax-patterned, and the electrodes were screen-printed on paper based substrate. (b) POC platform formed by clamping the paper-A and -B between board-A and -B with embedded electrical contacts. Reprinted from Biomaterials, 33, (Ge et al., 2012a), Copyright (2012), with permission from Elsevier.
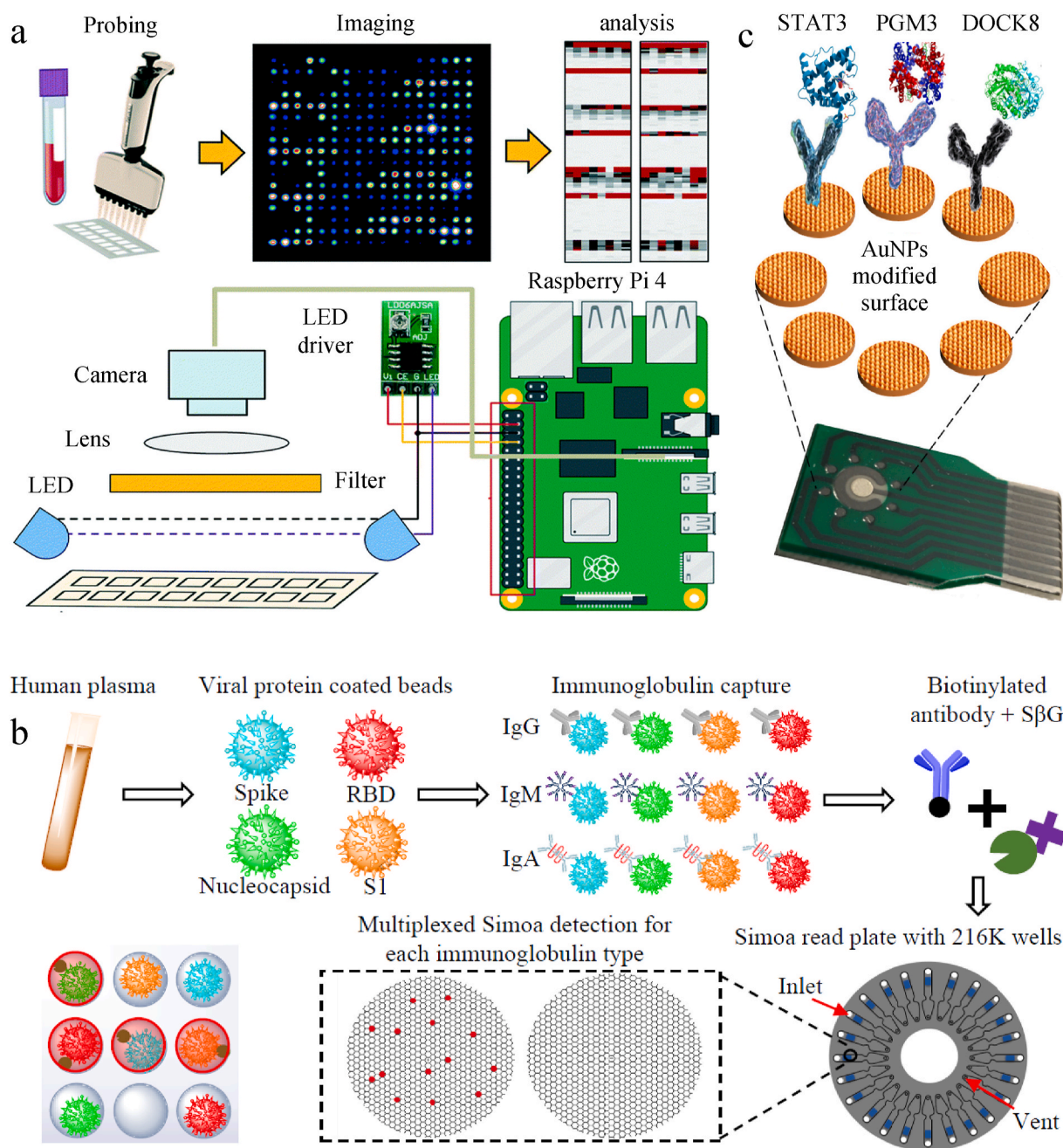
Fig. 9. Microarray based multiplexed immunosensors. (a) For optical microarrays, liquid samples are firstly plotted onto substrate, then images or optical signals will be recorded where the intensities of optical signals are normally proportional to the concentration of corresponding antibodies. Reproduced from (Hedde et al., 2020) with permission from the Royal Society of Chemistry. LED-illumination systems can be controlled with a single board computer. (b) Schematic of the Simoa technology in detecting IgG, IgM and IgA antibodies. S1: S1 subunit; RBD: receptor-binding domain; SβG: Streptavidin-β-galactosidase. (c) Schematic of electrochemical microarray based immunosensor for the simultaneous detection of signal transducer and activator of transcription 3 (STAT3), dedicator of cytokinesis 8 (DOCK8) or phosphoglucomutase 3 (PGM3) proteins. Reprinted from Biosens. Bioelectron., 117, (Eissa et al., 2018), Copyright (2018), with permission from Elsevier.

improve the integration level of the multiplexed units, the capabilities of multifunction, sensitivity and reproducibility, and the ease of use by non-expert frontline healthcare workers.

3.3. Microfluidics based lab-on-chip platform

The combination of highly integrated microarray platforms and the fast-developing microfluidic processing techniques have greatly pushed the boundaries of multiplexed POC immunosensors. This microfluidics based lab-on-chip platform mainly employs the spatial and particle based multiplexing strategy, and consists of microfluidics (either in

series or in parallel) made with photoresists, PDMS or other polymers, which accurately divert liquid samples to the detection or processing points using a variety of inlets or valves (Bange et al., 2005).

The simplest and most used function of a microfluidic device is to guide the liquid sample to the specific sensing arrays. As shown in Fig. 10 (a), such an immunosensor could include a single channel to direct the plasma sample perpendicularly flowing over the graphene FET array, where each device is functionalised by a different antibody for multiplexing purposes (Park et al., 2020). Upon the binding between antibodies and their specific biomarkers, the detection can be achieved via monitoring the change of electrical resistance or the shift of the Dirac
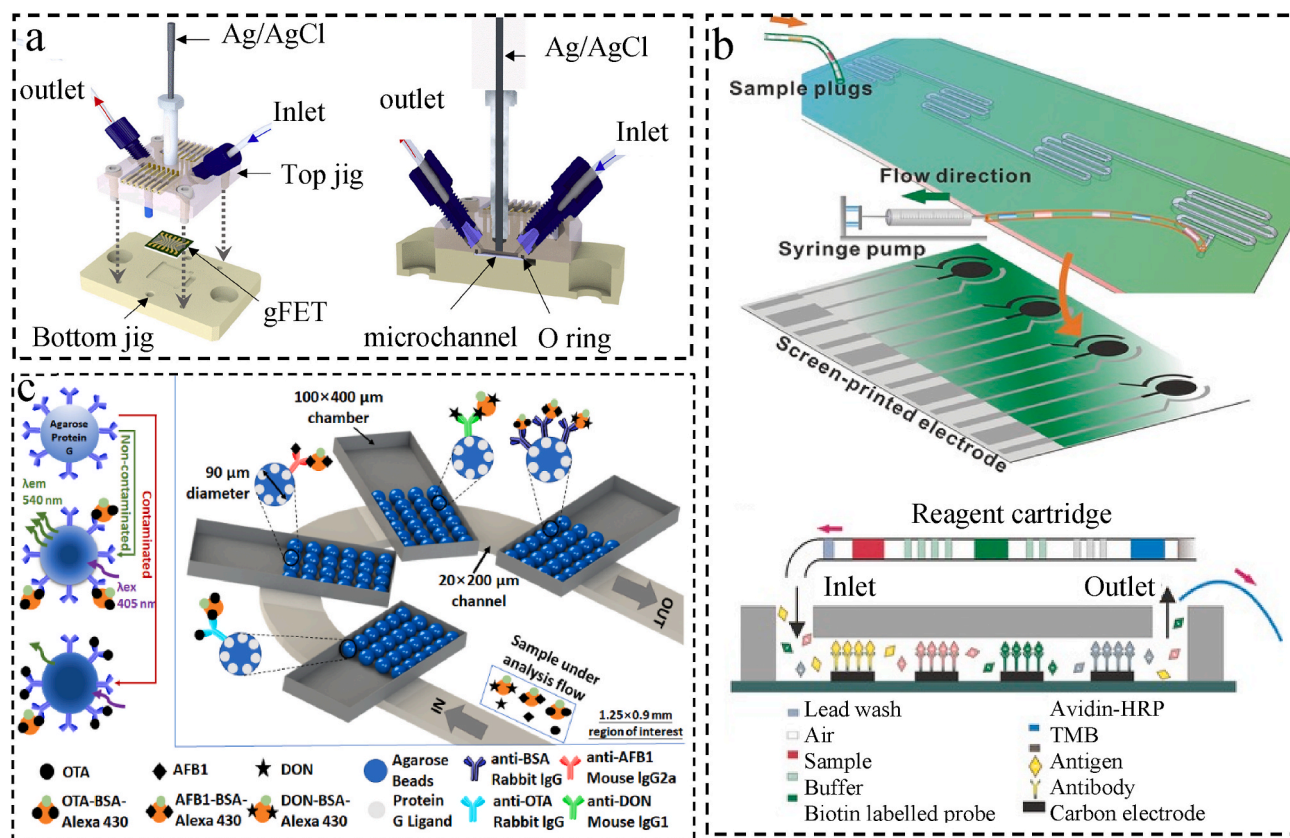
Fig. 10. Microfluidics based lab-on-chip multiplexed immunosensors. (a) The disassembled view of a multiplexed electrical immunosensor with a single guide microfluidic channel across the sensing array. Reprinted from Biosens. Bioelectron, 167, (Park et al., 2020), Copyright (2020), with permission from Elsevier. (b) Top: a microfluidic immunosensor containing all reagents in the PDMS layer for the simultaneous detection of four biomarkers. Reprinted by permission from Creative Commons Attribution CC BY License: John Wiley and Sons, Adv. Mater., (Yang et al., 2014), Copyright 2014. (c) A multiplexed microfluidic based fluorescence competitive immunosensor for the detection of three biomarkers in series with a portable readout platform. Reproduced from (Soares et al., 2018) with permission from the Royal Society of Chemistry.

point (Ramadan et al., 2021). More advanced electrical configuration may include channel networks (2–4 channels), actuation valves, and multiple inlets and outlets for each channel. For example, Liu's group developed an immunosensor platform with two parallel channels and sensing areas for the simultaneous detection of *Salmonella* serotypes B and D (Liu et al., 2019). Although this configuration of microfluidics can be further integrated for high-level multiplexing with more advanced fabrication techniques (Thorsen et al., 2002), it is not a practical application for POC diagnostic in the current set-up, due to its sensor complexity, bulky pneumatic control system, and complicated fluid connections.

Microfluidics is more frequently integrated and reported with electrochemical immunosensors than with the electrical approaches. These platforms can be categorised into many subtypes according to the number of labelled particles and the spatial strategies used for multiplexing purposes. For example, the detection of multiple biomarkers can be achieved using different redox particles in a single microfluidic channel (Zhou et al., 2010). However, its capability of multiplexed detection is normally limited by the number of particles that can be used in one sensing process. Multiplexed detection can also be realised using a single label in a single microfluidic channel, but with spatially separated electrodes. Yang and Otieno separately reported their representative microfluidics based platforms for the multiplexed detection of biomarkers (Otieno et al., 2016; Yang et al., 2014). Their setup uses an array of printed working electrodes, which has been functionalised with corresponding antibodies and can be addressed individually in a sealed microfluidic channel, as shown in Fig. 10 (b). HRP is one of the most used enzymes to label all detector antibodies in this configuration

(Serafín et al., 2020). This method offers the advantage of enhanced simplicity for the simultaneous detection of multiple biomarkers. In addition, multiplexed electrochemical immunosensing can be performed in a label-free manner, where the sensing mechanism relies on the change of the electrochemical response of the modified electrode surface (Cotchim et al., 2020), rather than enzymatic or redox tags.

Like electrical immunosensors, when multiple biomarkers need to be detected simultaneously in microfluidics, it is preferable to separate each sensing unit spatially to avoid the crosstalk caused by unavoidable lateral liquid movement, and to avoid the decreased target concentration with the longer flow trajectories. This is specifically important for highly integrated devices (Wilson and Nie, 2006b). One recent example presented a microfluidic electrochemical immunosensor for simultaneous detection of three different viruses (Han et al., 2016a). Their microfluidic system consisted of one single sample inlet, then branched into three parallel channels with their individual immunosensors embedded inside. Each device had its own working, counter, and reference electrode, which were all spatially separated to avoid any crosstalk.

Microfluidics based multiplexing can also be integrated with optical immunosensors. Fluorescence detection is the major type of multiplexed optical immunosensor with the potential to be used as POC diagnostic devices since the detection can be achieved using cost-effective and miniaturised photodiodes. Soares et al. reported a novel multiplexed microfluidic immunosensor, which consisted of four microfluidic channels with immobilised microbeads, one main microfluidic channel for sample injection, and an array of coupled photodiodes fluorescence signal acquisition, as shown in Fig. 10 (c) (Soares et al., 2018). The beads

in the first three chambers were functionalised with three different antibodies against their corresponding targets, whilst the beads in the fourth channel were modified with anti-Bovine serum albumin (BSA) antibodies to provide a maximum signal level (serves as a negative control). As the sample and mycotoxin-BSA-Alexa 430 composites flowed through the four channels in series, target biomarkers competed with the composites for binding to the antibodies on immobilised beads. The higher the biomarker concentration in the sample, the lower the fluorescence signal detected by their portable readout system. Along with this work, other microfluidic optical POC platforms have been created using different methods, such as chemiluminescence (Mou et al., 2019) and SPR (Tokel et al., 2015). More articles have been published on the multiplexed microfluidic immunosensor using other optical methods, such as electrochemiluminescence (Kadimisetty et al., 2018), magnetic bead assisted detection (Gao et al., 2019), SERS detection (Gao et al., 2018), or localised surface plasmon resonance (Yavas et al., 2018). However, the bulky optical setup and complexity of the devices reduce their potential and ease to be translated into frontline clinical settings as a POC device.

More importantly, microfluidics empowers immunosensors with dedicated sample processing and manipulation functionalities to achieve a fully integrated lab-on-chip platform. This enables detection in high viscosity, multiple components, biological samples with complex matrices, such as whole blood, which will eliminate the requirement of sample preparation and will promote the translation into frontline clinical settings. For example, Gao et al. developed a passive microfluidic collector to enable efficient wound fluid collection (Fig. 11 (a)). The collector consists of an array of half-open, sawtooth-shaped capillary to guide the body fluid flow directionally towards the sensors (Gao et al., 2021). Another important function for biological sample processing is the separation of the disrupting particles; this is normally the first step in conventional clinical assays, i.e., separating the plasma from whole blood, which requires a dedicated centrifuge and professional operation in laboratorial settings. Alternatively, the Zweifach-Fung effect can be employed together with cross flow and hydrodynamic flow methods in microfluidics for the simultaneous separation of plasma, red blood cells (RBC), and white blood cells (WBCs) from the finger prick blood, as demonstrated in Fig. 11 (b). The separation mechanism is that, when whole blood encounters a branch in a microfluidic channel, larger

particles preferably go into the channel with higher flow rate, whilst smaller particles (or liquid) concentrate in the channel with a lower flow rate. In addition to liquid collection and separation, microfluidics can also assist with extraction, fluid mixing, and purification, as thoroughly reviewed by Nge et al., (2013). These platforms could greatly promote biological sample analysis in resource-limited environments or POC settings. In summary, the roles of microfluidics in multiplexed POC immunosensors include controlling the flow conditions, reducing the sample volume, increasing the mixing rate of reagents, increasing the sensitivity of detection, and integrating multiple sample preparation functions towards a full lab-on-chip platform.

4. Conclusions and prospects

Since the rise of the multiplexed biosensing concept, many commercial products and prototype platforms have been reported using different multiplexing strategies and sensing platforms with their own advantages and drawbacks. Some of them, such as Simoa and the Proximity Extension Assay, have recently even become the new generation of gold standard laboratory tests. They have delivered promising results from primary studies using both artificial and clinical samples, and they have also started to show the significant impact on clinical diagnosis and discovery, and validation of biomarkers. However, none of these platforms can currently be deployed as POC diagnostic tools.

This leads to an emerging urgent need for multiplexed POC immunosensors, which should be produced in a cost-effective way, and should provide high sensitivity, rapid readout time, and low system complexity for minimally trained users. To respond to such a need, different strategies have been proposed for the development of multiplexed immunosensors, which mainly include spatial, time division, frequency division, barcoded, and particle based multiplexing as we discussed in this review. To allow these strategies to be used as POC applications, paper based, microarray based, and microfluidic based lab-on-chip platforms have been developed in parallel. Although preliminary results have been demonstrated in laboratories, many challenges remain for further translation and commercialization of these multiplexed immunosensors. Since most of them are still at the early development stage (lack of clinical results), limited by their multiplexing capability (only a low number of target biomarkers can be detected
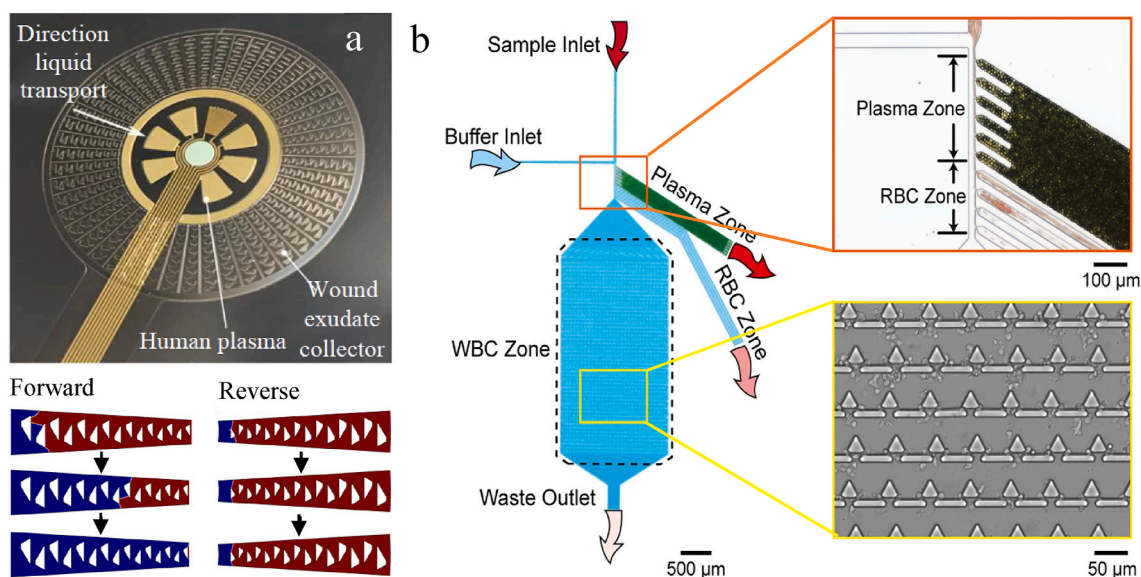

Fig. 11. Microfluidics with sample processing and manipulation functionalities. (a) Directional microfluidic wound exudate collector integrated with multiplexed electrochemical immunosensors. Reprinted by permission from Creative Commons CC BY License: Sci. Adv., (Gao et al., 2021), Copyright 2021. (b) Schematic of a blood component separation microfluidic device. The device can simultaneously separate plasma, RBCs, and WBCs through a single device. Reprinted by permission from Creative Commons CC BY License: Springer Nature, Sci. Rep., (Kuan et al., 2018), Copyright 2018.

simultaneously), or limited by high system complexity (microarray or microbead based platforms). Upon this, considerable effort should be put in the integration of other functional components (e.g., blood filtering or liquid manipulation) to minimise the user intervention. In addition, most of the current achievements focus on the sensing platform hardware. The multiplexing algorithms also need to be further developed and optimised for the combined signals to deal with matrix effects and patient-to-patient variations. As a summary, the future direction for the development of multiplexed immunosensors will be towards the standardization and miniaturization of the system components and to the highly smart integration as a ready-to-use application.

CRediT authorship contribution statement

Bruno Gil Rosa: Writing – original draft, Visualization. **Oluwatomi E. Akingbade:** Writing – original draft, Visualization. **Xiaotong Guo:** Writing – original draft, Visualization. **Laura Gonzalez-Macia:** Writing – review & editing. **Michael A. Crone:** Writing – review & editing. **Loren P. Cameron:** Writing – review & editing. **Paul Freemont:** Writing – review & editing. **Kwang-Leong Choy:** Writing – review & editing. **Firat Güder:** Writing – review & editing. **Eric Yeatman:** Writing – review & editing. **David J. Sharp:** Writing – review & editing. **Bing Li:** Conceptualization, Writing – original draft, Visualization, Supervision, Project administration, Funding acquisition.

Declaration of competing interest

The authors declare that they have no known conflicted financial interests or personal relationships that could have appeared to influence the work reported in this paper.

Acknowledgment

References

Abadian, A., Manesh, S.S., Ashtiani, S.J., 2017. Microfluid. Nanofluidics 21 (4), 65.
Alghamdi, A., Reynard, C., Morris, N., Moss, P., Jarman, H., Hardy, E., Harris, T., Horner, D., Parris, R., Body, R., 2020. Emerg. Med. J. 37 (4), 223–228.
Balakrishnan, K.R., Anwar, G., Chapman, M.R., Nguyen, T., Kesavaraju, A., Sohn, L.L., 2013. Lab Chip 13 (7), 1302.
Balakrishnan, K.R., Whang, J.C., Hwang, R., Hack, J.H., Godley, L.A., Sohn, L.L., 2015. Anal. Chem. 87 (5), 2988–2995.
Banaei, N., Foley, A., Houghton, J.M., Sun, Y., Kim, B., 2017. Nanotechnology 28 (45), 455101.
Bange, A., Halsall, H.B., Heineman, W.R., 2005. Biosens. Bioelectron. 20 (12), 2488–2503.
Carbonaro, A., Sohn, L.L., 2005. Lab Chip 5 (10), 1155.
Castaño-Guerrero, Y., Moreira, F.T.C., Sousa-Castillo, A., Correa-Duarte, M.A., Sales, M. G.F., 2021. Electrochim. Acta 366, 137377.
Chandra, P.E., Sokolove, J., Hipp, B.G., Lindstrom, T.M., Elder, J.T., Reveille, J.D., Eberl, H., Klause, U., Robinson, W.H., 2011. Arthritis Res. Ther. 13 (3), 1–13.
Chen, Z., Dodig-Crnković, T., Schwenk, J.M., Tao, S.-c., 2018. Clin. Proteomics 15 (1), 1–15.
Chikkaveeraiah, B.V., Bhirde, A.A., Morgan, N.Y., Eden, H.S., Chen, X., 2012. ACS Nano 6 (8), 6546–6561.
Contreras-Naranjo, J., Aguilar, O., 2019. Biosensors 9 (1), 15.
Cooper, J., Yazvenko, N., Peyvan, K., Maurer, K., Taitt, C.R., Lyon, W., Danley, D.L., 2010. PLoS One 5 (3), e9781.
Cotchim, S., Thavarungkul, P., Kanatharana, P., Limbut, W., 2020. Anal. Chim. Acta 1130, 60–71.
Dincer, C., Bruch, R., Kling, A., Dittrich, P.S., Urban, G.A., 2017. Trends Biotechnol. 35 (8), 728–742.
Dubois, B., Feldman, H.H., Jacova, C., Hampel, H., Molinuevo, J.L., Blennow, K., DeKosky, S.T., Gauthier, S., Selkoe, D., Bateman, R., Cappa, S., Crutch, S., Engelborghs, S., Frisoni, G.B., Fox, N.C., Galasko, D., Habert, M.-O., Jicha, G.A., Nordberg, A., Pasquier, F., Rabinovici, G., Robert, P., Rowe, C., Salloway, S., Sarazin, M., Epelbaum, S., de Souza, L.C., Vellas, B., Visser, P.J., Schneider, L., Stern, Y., Scheltens, P., Cummings, J.L., 2014. Lancet Neurol. 13 (6), 614–629.
Eissa, S., Abdulkarim, H., Dasouki, M., Al Mousa, H., Arnout, R., Al Saud, B., Rahman, A. A., Zourob, M., 2018. Biosens. Bioelectron. 117, 613–619.
Gao, R., Cheng, Z., Wang, X., Yu, L., Guo, Z., Zhao, G., Choo, J., 2018. Biosens. Bioelectron. 119, 126–133.
Gao, Y., Huo, W., Zhang, L., Lian, J., Tao, W., Song, C., Tang, J., Shi, S., Gao, Y., 2019. Biosens. Bioelectron. 123, 204–210.
Gao, Y., Nguyen, D.T., Yeo, T., Lim, S.B., Tan, W.X., Madden, L.E., Jin, L., Long, J.Y.K., Aloweni, F.A.B., Liew, Y.J.A., 2021. Sci. Adv. 7 (21), eabg9614.
Ge, L., Yan, J., Song, X., Yan, M., Ge, S., Yu, J., 2012a. Biomaterials 33 (4), 1024–1031.
Ge, S., Ge, L., Yan, M., Song, X., Yu, J., Huang, J., 2012b. Chem. Commun. 48 (75), 9397.
Hampel, H., O'Bryant, S.E., Molinuevo, J.L., Zetterberg, H., Masters, C.L., Lista, S., Kiddle, S.J., Batrla, R., Blennow, K., 2018. Nat. Rev. Neurol. 14 (11), 639–652.
Han, J.-H., Lee, D., Chew, C.H.C., Kim, T., Pak, J.J., 2016a. Sensor. Actuator. B Chem. 228, 36–42.
Han, Y., Wu, H., Liu, F., Cheng, G., Zhe, J., 2014. Anal. Chem. 86 (19), 9717–9722.
Han, Y., Wu, H., Liu, F., Cheng, G., Zhe, J., 2016b. Biomicrofluidics 10 (2), 024109.
Hedde, P.N., Abram, T.J., Jain, A., Nakajima, R., de Assis, R.R., Pearce, T., Jasinskas, A., Toosky, M.N., Khan, S., Felgner, P.L., 2020. Lab Chip 20 (18), 3302–3309.
Hossain, S.Z., Ozimok, C., Sicard, C., Aguirre, S.D., Ali, M.M., Li, Y., Brennan, J.D., 2012. Anal. Bioanal. Chem. 403 (6), 1567–1576.
Jagtiani, A.V., Carletta, J., Zhe, J., 2011. J. Micromech. Microeng. 21, 065004.
Jia, X., Liu, Z., Liu, N., Ma, Z., 2014. Biosens. Bioelectron. 53, 160–166.
Jichun, Z., Yue, H., Trombly, N., Chao, Y., Mason, A., 2005. IEEE Sensor. J.
Jin, Y., Chen, Q., Luo, S., He, L., Fan, R., Zhang, S., Yang, C., Chen, Y., 2021. Food Chem. 336, 127718.
Jirakova, L., Hrstka, R., Campuzano, S., Pingarrón, J.M., Bartosik, M., 2019. Electroanalysis 31 (2), 293–302.
Kadimisetty, K., Malla, S., Bhalerao, K.S., Mosa, I.M., Bhakta, S., Lee, N.H., Rusling, J.F., 2018. Anal. Chem. 90 (12), 7569–7577.
Kadimisetty, K., Malla, S., Sardesai, N.P., Joshi, A.A., Faria, R.C., Lee, N.H., Rusling, J.F., 2015. Anal. Chem. 87 (8), 4472–4478.
Khetani, S., Ozhukil Kollath, V., Kundra, V., Nguyen, M.D., Debert, C., Sen, A., Karan, K., Sanati-Nezhad, A., 2018. ACS Sens. 3 (4), 844–851.
Kim, K., Hall, D.A., Yao, C., Lee, J.-R., Ooi, C.C., Bechstein, D.J.B., Guo, Y., Wang, S.X., 2018. Sci. Rep. 8 (1).
Kim, K., Kim, M.-J., Kim, S.Y., Park, S., Park, C.B., 2020. Nat. Commun. 11 (1), 1–9.
Koczula, K.M., Gallotta, A., 2016. Essays Biochem. 60 (1), 111–120.
Kuan, D.-H., Wu, C.-C., Su, W.-Y., Huang, N.-T., 2018. Sci. Rep. 8 (1), 1–9.
Layqah, L.A., Eissa, S., 2019. Microchim. Acta 186 (4), 1–10.
Lee, H., Ugay, D., Hong, S., Kim, Y., 2020. Dement. Neurocogn. Disord. 19 (1), 1.
Lee, H.J., Nedelkov, D., Corn, R.M., 2006. Anal. Chem. 78 (18), 6504–6510.
Lee, H.J., Roh, Y.H., Kim, H.U., Kim, S.M., Bong, K.W., 2019. Lab Chip 19 (1), 111–119.
Li, B., Pan, G., Avent, N.D., Lowry, R.B., Madgett, T.E., Waines, P.L., 2015. Biosens. Bioelectron. 72, 313–319.
Li, B., Pan, G., Suhail, A., Islam, K., Avent, N., Davey, P., 2017. Carbon 118, 43–49. htt ps://doi.org/10.1021/acssensors.1c02232.
Li, B., Tan, H., Anastasova, S., Power, M., Seichepine, F., Yang, G.-Z., 2019. Biosens. Bioelectron. 123, 77–84.
Li, B., Tan, H., Jenkins, D., Srinivasa Raghavan, V., Rosa, B.G., Güder, F., Pan, G., Yeatman, E., Sharp, D.J., 2020. Carbon 168, 144–162.
Li, B., Zhang, G., Tahirbegi, I.B., Morten, M.J., Tan, H., 2021. Electrochem. Commun. 123, 106927.
Li, J., Macdonald, J., 2016a. Lab Chip 16 (2), 242–245.
Li, J., Macdonald, J., 2016b. Biosens. Bioelectron. 83, 177–192.
Liang, J., Jiang, N., Zhou, S., Wang, X., Xu, Y., Wu, C., Kirsanov, D., Legin, A., Wan, H., Wang, P., 2021. Anal. Chim. Acta 338603.
Lim, W.Y., Thevarajah, T.M., Goh, B.T., Khor, S.M., 2019. Biosens. Bioelectron. 128, 176–185.
Lin, C., Ryder, L., Probst, D., Caplan, M., Spano, M., Labelle, J., 2017. Biosens. Bioelectron. 89, 743–749.
Lisowski, P., Zarzycki, P.K., 2013. Chromatographia 76 (19), 1201–1214.
Liu, B., Zhang, D., Ni, H., Wang, D., Jiang, L., Fu, D., Han, X., Zhang, C., Chen, H., Gu, Z., 2018a. ACS Appl. Mater. Interfaces 10 (1), 21–26.
Liu, F., Kc, P., Ni, L., Zhang, G., Zhe, J., 2018b. Organogenesis 14 (2), 67–81.
Liu, F., Ni, L., Zhe, J., 2018c. Biomicrofluidics 12 (2), 021501.
Liu, J., Jasim, I., Shen, Z., Zhao, L., Dweik, M., Zhang, S., Almasri, M., 2019. PLoS One 14 (5), e0216873.
Liu, R., Wang, N., Kamili, F., Sarioglu, A.F., 2016. Lab Chip 16 (8), 1350–1357.
Mahato, K., Kumar, S., Srivastava, A., Maurya, P.K., Singh, R., Chandra, P., 2018. Electrochemical Immunosensors. Elsevier, pp. 359–414.
Mao, X., Baloda, M., Gurung, A.S., Lin, Y., Liu, G., 2008. Electrochem. Commun. 10 (10), 1636–1640.
Martinez, A.W., Phillips, S.T., Whitesides, G.M., 2008. P. Natl. Acad. Sci. USA 105 (50), 19606–19611.
Meissner, R., Joris, P., Eker, B., Bertsch, A., Renaud, P., 2012. Lab Chip 12 (15), 2712.
Mohammed, M.-I., Desmulliez, M.P., 2011. Lab Chip 11 (4), 569–595.
Molderez, T.R., Prévoteau, A., Ceyssens, F., Verhelst, M., Rabaey, K., 2021. Biosens. Bioelectron. 174, 112813.
Moral-Vico, J., Barallat, J., Abad, L., Olivé-Monllau, R., Muñoz-Pascual, F.X., Galán Ortega, A., Del Campo, F.J., Baldrich, E., 2015. Biosens. Bioelectron. 69, 328–336.
Mou, L., Dong, R., Hu, B., Li, Z., Zhang, J., Jiang, X., 2019. Lab Chip 19 (16), 2750–2757.
Nge, P.N., Rogers, C.I., Woolley, A.T., 2013. Chem. Rev. 113 (4), 2550–2583.
Noguera, P., Posthuma-Trumpie, G., Van Tuil, M., Van der Wal, F., De Boer, A., Moers, A., Van Amerongen, A., 2011. Anal. Bioanal. Chem. 399 (2), 831–838.

Norman, M., Gilboa, T., Ogata, A.F., Maley, A.M., Cohen, L., Busch, E.L., Lazarovits, R., Mao, C.-P., Cai, Y., Zhang, J., 2020. Nat. Biomed. Eng. 4 (12), 1180–1187.

Otieno, B.A., Krause, C.E., Jones, A.L., Kremer, R.B., Rusling, J.F., 2016. Anal. Chem. 88 (18), 9269–9275.

Park, D., Kim, J.H., Kim, H.J., Lee, D., Lee, D.S., Yoon, D.S., Hwang, K.S., 2020. Biosens. Bioelectron. 167, 112505.

Peters, K.L., Corbin, I., Kaufman, L.M., Zreibe, K., Blanes, L., McCord, B.R., 2015. Anal. Methods 7 (1), 63–70.

Petrova, I., Konopsky, V., Nabiev, I., Sukhanova, A., 2019. Sci. Rep. 9 (1), 1–9.

Phillips, E.A., Young, A.K., Albarran, N., Butler, J., Lujan, K., Hamad-Schifferli, K., Gomez-Marquez, J., 2018. Adv. Healthc. Mater. 7 (14), 1800104.

Pollock, N.R., Rolland, J.P., Kumar, S., Beattie, P.D., Jain, S., Noubary, F., Wong, V.L., Pohlmann, R.A., Ryan, U.S., Whitesides, G.M., 2012. Sci. Transl. Med. 4 (152), 152ra129.

Prakash, S., Ashley, B.K., Doyle, P.S., Hassan, U., 2020. Sci. Rep. 10 (1), 1–10.

Ramadan, S., Lobo, R., Zhang, Y., Xu, L., Shaforost, O., Kwong Hong Tsang, D., Feng, J., Yin, T., Qiao, M., Rajeshirke, A., 2021. ACS Appl. Mater. Interfaces 13 (7), 7854–7864.

Rissin, D.M., Kan, C.W., Campbell, T.G., Howes, S.C., Fournier, D.R., Song, L., Piech, T., Patel, P.P., Chang, L., Rivnak, A.J., 2010. Nat. Biotechnol. 28 (6), 595–599.

Roda, A., Cavalera, S., Di Nardo, F., Calabria, D., Rosati, S., Simoni, P., Colitti, B., Baggiani, C., Roda, M., Anfossi, L., 2021. Biosens. Bioelectron. 172, 112765.

Rosser, C.J., Dai, Y., Miyake, M., Zhang, G., Goodison, S., 2014. BMC Biotechnol. 14 (1), 1–6.

Ruan, X., Wang, Y., Kwon, E.Y., Wang, L., Cheng, N., Niu, X., Ding, S., Van Wie, B.J., Lin, Y., Du, D., 2021. Biosens. Bioelectron. 184, 113238.

Sankhala, D., Muthukumar, S., Prasad, S., 2018. SLAS Technol 23 (6), 529–539.

Serafín, V., Razzino, C.A., Gamella, M., Pedrero, M., Povedano, E., Montero-Calle, A., Barderas, R., Calero, M., Lobo, A.O., Yáñez-Sedeño, P., 2020. Anal. Bioanal. Chem. 1–13.

Sheridan, C., 2020. Nat. Biotechnol. 38 (5), 515–518.

Soares, R.R., Santos, D.R., Pinto, I.F., Azevedo, A.M., Aires-Barros, M.R., Chu, V., Conde, J.P., 2018. Lab Chip 18 (11), 1569–1580.

Soler, M., Belushkin, A., Cavallini, A., Kebbi-Beghdadi, C., Greub, G., Altug, H., 2017. Biosens. Bioelectron. 94, 560–567.

Taranova, N., Berlina, A., Zherdev, A., Dzantiev, B., 2015. Biosens. Bioelectron. 63, 255–261.

Thorsen, T., Maerkl, S.J., Quake, S.R., 2002. Science 298 (5593), 580–584.

Tokel, O., Yildiz, U.H., Inci, F., Durmus, N.G., Ekiz, O.O., Turker, B., Cetin, C., Rao, S., Sridhar, K., Natarajan, N., 2015. Sci. Rep. 5 (1), 1–9.

Tsai, T.-T., Huang, T.-H., Ho, N.Y.-J., Chen, Y.-P., Chen, C.-A., Chen, C.-F., 2019. Sci. Rep. 9 (1), 1–8.

Vaidyanathan, R., Van Leeuwen, L.M., Rauf, S., Shiddiky, M.J.A., Trau, M., 2015. Sci. Rep. 5 (1), 9756.

Wan, Y., Su, Y., Zhu, X., Liu, G., Fan, C., 2013. Biosens. Bioelectron. 47, 1–11.

Wang, D., He, S., Wang, X., Yan, Y., Liu, J., Wu, S., Liu, S., Lei, Y., Chen, M., Li, L., 2020. Nat. Biomed. Eng. 1–9.

Wang, K., Wadhwa, P.D., Culhane, J.F., Nelson, E.L., 2005. J. Reprod. Immunol. 66 (2), 175–191.

Wang, N., Liu, R., Asmare, N., Chu, C.-H., Sarioglu, A.F., 2021. Biosens. Bioelectron. 174, 112818.

Wilson, M.S., Nie, W., 2006a. Anal. Chem. 78 (8), 2507–2513.

Wilson, M.S., Nie, W., 2006b. Anal. Chem. 78 (18), 6476–6483.

Wood, D., Braun, G., Fraikin, J.-L., Swenson, L., Reich, N., Cleland, A., 2007. Lab Chip 7 (4), 469–474.

Wu, D., Rios-Aguirre, D., Chounlakone, M., Camacho-Leon, S., Voldman, J., 2018. Biosens. Bioelectron. 117, 522–529.

Wu, H., Han, Y., Yang, X., Chase, G.G., Tang, Q., Lee, C.-J., Cao, B., Zhe, J., Cheng, G., 2015. PLoS One 10 (2), e0115046.

Wu, J., Yan, F., Tang, J., Zhai, C., Ju, H., 2007. Clin. Chem. 53 (8), 1495–1502.

Xianyu, Y., Wu, J., Chen, Y., Zheng, W., Xie, M., Jiang, X., 2018. Angew. Chem. Int. Ed. 57 (25), 7503–7507.

Xu, L., Li, D., Ramadan, S., Li, Y., Klein, N., 2020. Biosens. Bioelectron., 112673

Yang, C., Huang, Y., Hassler, B.L., Worden, R.M., Mason, A.J., 2009. IEEE T. Biomed. Circ. Sys. 3 (3), 160–168.

Yang, F., Zuo, X., Li, Z., Deng, W., Shi, J., Zhang, G., Huang, Q., Song, S., Fan, C., 2014. Adv. Mater. 26 (27), 4671–4676.

Yang, M., Zhang, W., Zheng, W., Cao, F., Jiang, X., 2017. Lab Chip 17 (22), 3874–3882.

Yavas, O., Aćimović, S.S., Garcia-Guirado, J., Berthelot, J., Dobosz, P., Sanz, V., Quidant, R., 2018. ACS Sens. 3 (7), 1376–1384.

Zhao, C., Thuo, M.M., Liu, X., 2013. Sci. Technol. Adv. Mater. 14 (5), 054402.

Zhao, X., Wang, J., Chen, H., Xu, H., Bai, L., Wang, W., Yang, H., Wei, D., Yuan, B., 2019. Sensor. Actuator. B Chem. 301, 127071.

Zheng, G., Patolsky, F., Cui, Y., Wang, W.U., Lieber, C.M., 2005. Nat. Biotechnol. 23 (10), 1294–1301.

Zhou, F., Lu, M., Wang, W., Bian, Z.-P., Zhang, J.-R., Zhu, J.-J., 2010. Clin. Chem. 56 (11), 1701–1707.

Zupančič, U., Jolly, P., Estrela, P., Moschou, D., Ingber, D.E., 2021. Adv. Funct. Mater. 31 (16), 2010638.